PROJECT REPORT

On

ELECTROSPUN MEMBRANES IMPREGNATED WITH ZnO/MXene FOR WATER TREATMENT

Submitted by,

SWITLANA MARIYA JOHN (AM23CHE014)

In partial fulfillment for the award of the Post graduate Degree in Chemistry

DEPARTMENT OF CHEMISTRY
AND
CENTRE FOR RESEARCH

ST. TERESA'S COLLEGE (AUTONOMOUS)
ERNAKULAM

2024-2025

DEPARTMENT OF CHEMISTRY
AND
CENTRE FOR RESEARCH

ST. TERESA'S COLLEGE (AUTONOMOUS)

ERNAKULAM

M.Sc. CHEMISTRY PROJECT REPORT

Name : **SWITLANA MARIYA JOHN**
Register Number : **AM23CHE014**
Year of Work : **2024-2025**

This is to certify that the project "**ELECTROSPUN MEMBRANES IMPREGNATED WITH ZnO/MXene FOR WATER TREATMENT**" is the work done by **SWITLANA MARIYA JOHN .**

Dr. Saritha Chandran A.
Head of the Department

Dr. Nisha T Padmanabhan
Staff-member in charge

Submitted to the Examination of Master's degree in Chemistry

Date: 30/4/25

Examiners: Dr. Deepa C S

Dr. Roy Rajan Paul

ST.TERESA'S COLLEGE (AUTONOMOUS)
ERNAKULAM

Certificate of Plagiarism Check for Dissertation

Author Name	SWITLANA MARIYA JOHN , JEENA SAJI
Course of Study	M.Sc. Chemistry
Name of Guide	Dr. Nisha T P
Department	Chemistry & Centre For Research
Acceptable Maximum Limit	20
Submitted By	library@teresas.ac.in
Paper Title	ELECTROSPUN MEMBRANES IMPREGNATED WITH ZnO/MXene FOR WATER TREATMENT
Similarity	9% AI - 5%
Paper ID	3421936
Total Pages	111
Submission Date	2025-03-21 14:25:26

Signature of Student

Signature of Guide

Checked By
College Librarian

ST. TERESA'S COLLEGE LIBRARY ERNAKULAM

DEPARTMENT OF CHEMISTRY
AND
CENTRE FOR RESEARCH

ST. TERESA'S COLLEGE (AUTONOMOUS)

ERNAKULAM

CERTIFICATE

This is to certify that the project work titled "**ELECTROSPUN MEMBRANES IMPREGNATED WITH ZnO/MXene FOR WATER TREATMENT**" is the work done by **SWITLANA MARIYA JOHN** under the guidance of **Dr. Nisha T Padmanabhan, Assistant professor,** Department of Chemistry and Centre for Research, St. Teresa's College, Ernakulam in partial fulfilment of the award of the Degree of Master of Science in Chemistry at St. Teresa's College, Ernakulam affiliated to Mahatma Gandhi University, Kottayam.

Dr. Nisha T Padmanabhan

Assistant professor

Dr. Saritha Chandran A.

Head of the Department

DEPARTMENT OF CHEMISTRY
AND
CENTRE FOR RESEARCH

ST. TERESA'S COLLEGE (AUTONOMOUS)

ERNAKULAM

CERTIFICATE

This is to certify that the project work titled "**ELECTROSPUN MEMBRANES IMPREGNATED WITH ZnO/MXene FOR WATER TREATMENT**" is the work done by **SWITLANA MARIYA JOHN** under the guidance of **Dr. Nisha T Padmanabhan, Assistant professor,** Department of Chemistry and Centre for Research, St. Teresa's College, Ernakulam in partial fulfilment of the award of the Degree of Master of Science in Chemistry at St. Teresa's College, Ernakulam affiliated to Mahatma Gandhi University, Kottayam.

Dr. Nisha T Padmanabhan
Assistant professor

Dr. Saritha Chandran A.
Head of the Department

DECLARATION

I hereby declare that the project work entitled "**ELECTROSPUN MEMBRANES IMPREGNATED WITH ZnO/MXene FOR WATER TREATMENT**" submitted to Department of Chemistry and Centre for Research, St. Teresa's College (Autonomous) affiliated to Mahatma Gandhi University, Kottayam, Kerala is a record of an original work done by me under the guidance of **Dr. Nisha T Padmanabhan, Assistant professor**, Department of Chemistry and Centre for Research, St. Teresa's College (Autonomous), Ernakulam (Internal Guide) This project work is submitted in the partial fulfillment of the requirements for the award of the Degree of Master of Science in Chemistry.

SWITLANA MARIYA JOHN

Acknowledgements

We are very grateful to God Almighty for his continuous blessings for the successful completion of my project.

We would like to express our profound sense of gratitude to Dr. Nisha T Padmanabhan, Assistant Professor, Department of Chemistry and Centre for Research, St. Teresa's College for her co-supervision, valuable guidance, personal attention, meaningful suggestions, help, and encouragement, throughout the execution of this project

We express our gratitude to Inter University Centre for Nanomaterials and Devices (IUCND), CUSAT, for providing the necessary facilities and support for this study throughout the project also the research scholars and non teaching staffs for their support, suggestions and help throughout the project.

I thank Dr. Saritha Chandran, HOD, Department of Chemistry and Centre for Research, for providing an opportunity to do the project and giving all support and guidance which helped me complete the project duly.(1)

I would also like to express my heartfelt gratitude to all our teachers and non-teaching staff of the Department for their wholehearted help throughout my project.

We are grateful to Dr. Alphonsa Vijaya Joseph, Principal, St. Teresa's College, for her support and providing good infrastructure for the study and development of students.

We would like to express our gratitude towards Rev. Sr. Nilima, Manager CSST, and Rev. Sr. Francis Ann, Director for their constant support and inspiration.

We heartily thank STIC (CUSAT) for providing facilities towards the characterization of the samples within the time limit, and under subsidized charges.

Last, but not least, we are grateful to our loving families and friends for the care, support.

Switlana Mariya John

Contents

Chapter 1

Introduction

Water pollution has increased substantially over the past few years. The graph is linearly increasing from the yearly 18th century and can be due to the underlying factors and the contribution of dyes in it.(2)In this work we concentrate how to adsorb the dyes released into aquatic environment and create a membrane which could actually adsorb the dye.(2)

Fig 1.1 Industrial wastewater pollution causing excessive foaming in a river under a bridge. The distinct purple coloration indicates possible contamination from synthetic dyes or chemical effluents, highlighting severe environmental degradation and water quality concerns. Reprinted from reference *(3)*

Water pollution occurs when harmful substances—often chemicals or microorganisms—contaminate a stream, river, lake, ocean, aquifer, or other body of water, degrading water quality and rendering it toxic to humans or the environment. This widespread problem of water pollution is jeopardizing our health. Unsafe water kills more people each year than war and all other forms of violence combined. Meanwhile, our drinkable water sources are finite: Less than 1 percent of the earth's freshwater is actually accessible to us. Without action, the challenges will only increase by 2050, when global demand for freshwater is expected to be one-third greater than it is now.

1.1 CAUSES OF WATER POLLUTION

Fig 1.2 Environmental impact of textile and industrial wastewater discharge. The images depict severe water pollution, including dye-contaminated effluents, aquatic ecosystem degradation, and industrial emissions, emphasizing the urgent need for sustainable wastewater management.

Water is uniquely vulnerable to pollution. Known as a “universal solvent,” water is able to dissolve more substances than any other liquid on earth. It’s the reason we have Kool-Aid and brilliant blue waterfalls. It’s also why water is so easily polluted. (4)Toxic substances from farms, towns, and factories readily dissolve into and mix with it, causing water pollution. Some of the major sources of water pollution worldwide includes: -

1.1.1 Excessive use of pesticides and fertilizer

The agricultural sector is both the largest consumer of global freshwater, utilizing around 70% of the Earth's surface water for farming and livestock, and a major contributor to water pollution. Around the world, agriculture is the leading cause of water degradation. In the United States, agricultural pollution is the top source of contamination in rivers and streams, the second-biggest source in wetlands, and the third main source in lakes. It’s also a major contributor of contamination to estuaries and groundwater.(5) Every time it rains, fertilizers, pesticides, and animal waste from farms and livestock operations wash nutrients and pathogens—such bacteria and viruses—into our waterways. Nutrient pollution, caused by excess nitrogen and phosphorus in water or air, is the number-one threat to water quality worldwide and can cause algal blooms, a toxic soup of blue-green algae that can be harmful to people and wildlife.

1.1.2 Sewage and wastewater

Used water is wastewater. It comes from our sinks, showers, and toilets (think sewage) and from commercial, industrial, and agricultural activities (think metals, solvents, and toxic sludge). The term also includes stormwater runoff, which occurs when rainfall carries road salts, oil, grease, chemicals, and debris from impermeable surfaces into our waterways.(6)These facilities reduce the amount of pollutants such as pathogens, phosphorus, and nitrogen in sewage, as well as heavy metals and toxic chemicals in industrial waste, before discharging the treated waters back into waterways. That's when all goes well. But according to Environmental Protection Act. Estimates, our nation's aging and easily overwhelmed sewage treatment systems also release more than 850 billion gallons of untreated wastewater each year.

1.1.3 Oil pollution

Big spills may dominate headlines, but consumers account for the vast majority of oil pollution in our seas, including oil and gasoline that drips from millions of cars and trucks every day. Moreover, nearly half of the estimated 1 million tons of oil that makes its way into marine environments each year comes not from tanker spills but from land-based sources such as factories, farms, and cities. At sea, tanker spills account for about 10 percent of the oil in waters around the world, while regular operations of the shipping industry through both legal and illegal discharges contribute about one-third. Oil is also naturally released from under the ocean floor through fractures known as seeps.(7)

1.1.4 Radioactive substances

Radioactive waste is any pollution that emits radiation beyond what is naturally released by the environment. It's generated by uranium mining, nuclear power plants, and the production and testing of military weapons, as well as by universities and hospitals that use radioactive materials for research and medicine. Radioactive waste can persist in the environment for thousands of years, making disposal a major challenge. Accidentally released or improperly disposed of contaminants threaten groundwater, surface water, and marine resources.

1.2 ADVERSE EFFECTS OF WATER POLLUTION ON HUMAN HEALTH

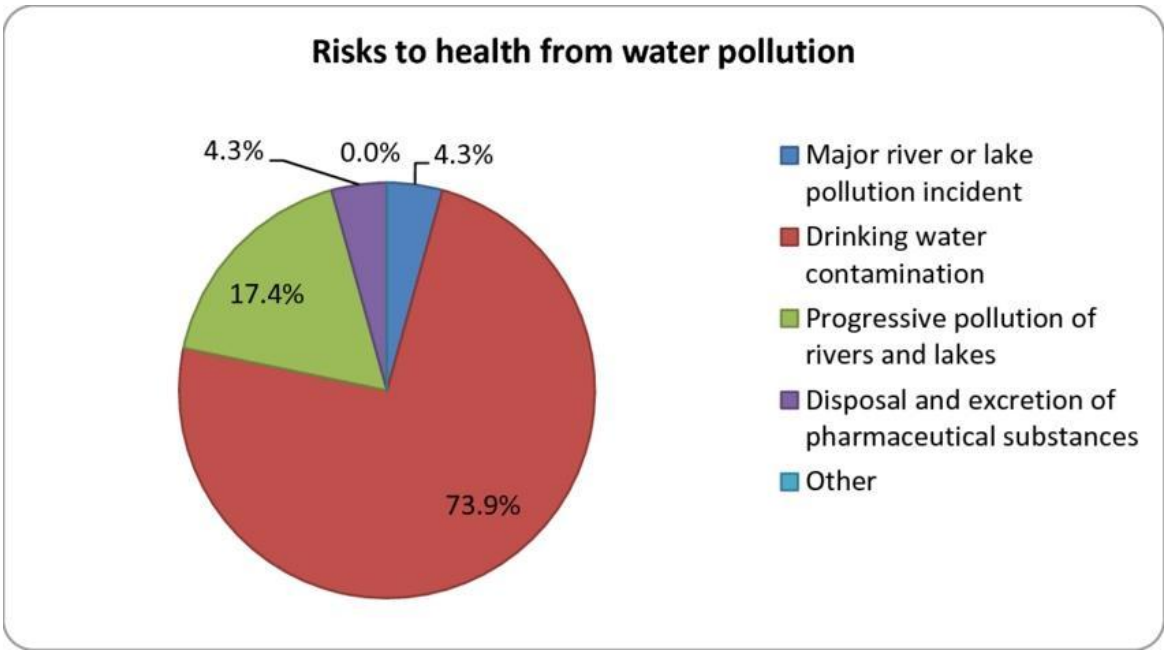

***Fig 1.3 The major contributors in the health risks associated with water pollution. Reprinted from reference** (7).*

To put it bluntly: Water pollution kills. In fact, it caused 1.8 million deaths in 2015, according to a study published in *The Lancet*.(9)Contaminated water can also make you ill. Every year, unsafe water sickens about 1 billion people. And low-income communities are disproportionately at risk because their homes are often closest to the most polluting industries.

Waterborne pathogens, in the form of disease-causing bacteria and viruses from human and animal waste, are a major cause of illness from contaminated drinking water. Diseases spread by unsafe water include cholera, giardia, and typhoid. Even in wealthy nations, accidental or illegal releases from sewage treatment facilities, as well as runoff from farms and urban areas, contribute harmful pathogens to waterways. (10)

1.3 GENERATION OF PHOTOCATALYST

Photocatalysts are the materials which can alter the rate of reaction on the exposure of light. This phenomenon is called photocatalysis. All photo catalyst are semiconductors. When a semiconductor is exposed to sunlight electrons from valence band get excited to conduction band. Now, holes are retained in valence band and electrons are present in conduction band.(11)

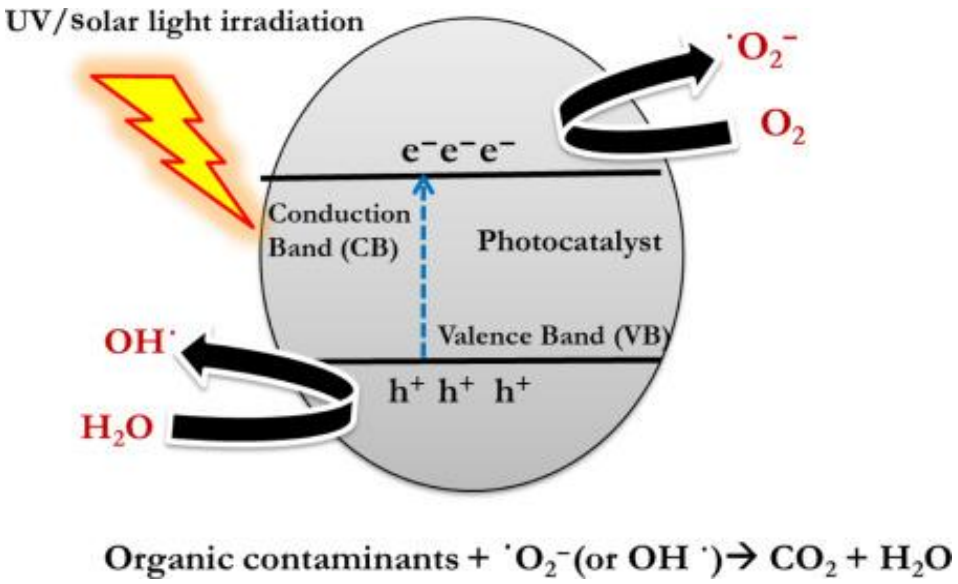

Fig 1.4 Schematic representation of the photocatalytic degradation mechanism. Under UV/solar light irradiation, electron-hole pairs are generated in the photocatalyst, leading to the formation of reactive oxygen species (·O_2^- and OH^-). These reactive species facilitate the degradation of organic contaminants into CO_2 and H_2O, demonstrating the efficiency of photocatalysis in water purification. Reprinted from reference *(12)*

There are two types of photocatalysts: -

1. Homogenous photocatalysts- when both semiconductors and reactants are in same phase like (gas, liquid, solid).

2. Hetrogenous photocatalysts- Semiconductors and reactants are in different face.

1.3.1 WATER TREATMENT BY PHOTOCATALYSIS

Photocatalytic water treatment methods primarily involve exposing polluted water to a semiconductor photocatalyst like titanium dioxide (TiO_2) under light irradiation, which generates highly reactive oxygen species (ROS) that break down organic pollutants into harmless byproducts; different approaches include: suspension photocatalysis, **i**mmobilized photocatalysis, membrane-based photocatalysis, solar-driven photocatalysis, and hybrid systems that combine photocatalysis with other water treatment techniques like filtration or biological processes. (13)

Key aspects of photocatalytic water treatment methods:

Photocatalyst selection:

- Titanium dioxide (TiO_2): Most commonly used due to its high efficiency, stability, and low cost.
- Other semiconductors: Zinc oxide (ZnO), tungsten trioxide (WO_3), cadmium sulfide (CdS), etc., can be used depending on the pollutant and desired light absorption range.

Light source:

- UV light: Most effective for TiO_2, but requires additional energy input.

- Visible light: Development of visible light-active photocatalysts is crucial for practical applications.
- Solar light: Utilizing natural sunlight for a sustainable approach.

Different photocatalytic treatment methods:

Suspension photocatalysis:

- Powdered photocatalyst is suspended in the water and exposed to light.
- Advantages: Simple setup, good for initial testing.
- Disadvantages: Difficult separation of catalyst particles from treated water, potential for secondary pollution.

Immobilized photocatalysis:

- Photocatalyst is fixed on a support material like glass beads, fibers, or membranes.
- Advantages: Easier catalyst separation, potential for continuous flow systems.
- Disadvantages: May require additional processing to immobilize the catalyst.

Membrane-based photocatalysis:

- Photocatalyst is integrated into a membrane filter for simultaneous filtration and photocatalytic degradation.
- Advantages: High efficiency for removing both particulate matter and dissolved pollutants.
- Disadvantages: Complex design and potential for membrane fouling.

Solar-driven photocatalysis:

- Utilizing sunlight as the light source for photocatalytic reactions.
- Advantages: Sustainable and environmentally friendly.
- Disadvantages: Dependence on weather conditions, potential for low efficiency.

Applications of photocatalytic water treatment:

- Removal of organic pollutants: Dyes, pesticides, pharmaceuticals, personal care products, and industrial waste.
- Degradation of heavy metals: Oxidation of heavy metals to less toxic forms.
- Disinfection of water: Inactivation of bacteria and viruses.

- Treatment of wastewater: Removal of pollutants from industrial and municipal

1.4. ZINC OXIDE AS A PHOTOCATALYST

Zinc oxide (ZnO) has many properties, including:

- **Chemical**: ZnO is an amphoteric oxide, meaning it has properties of both acids and bases. It's insoluble in water but dissolves in acids and alkalis.

- **Thermal**: ZnO has a high heat capacity and thermal conductivity, and a low thermal expansion coefficient. It has a high melting point of 1975°C, where it also decomposes.

- **Electrical**: ZnO has a large direct bandgap of about 3.3 eV at room temperature. It can withstand high electric fields and has lower electronic noise.

- **Structural**: ZnO exists in two common crystalline forms: wurtzite and zincblende.

- **Optical**: ZnO is thermochromic, meaning its color changes from white to yellow when heated in the presence of air, and back to white when cooled.

- **Hardness**: ZnO is moderately soft on the Mohs scale, with a hardness of about 4.5.

- **Elasticity**: ZnO's elastic constants are lower than those of related III-V semiconductors.

Pure ZnO is a white powder. However, in nature, it occurs as the rare mineral zincite, which usually contains manganese and other impurities that confer a yellow to red color. Crystalline ZnO is thermochromic, changing from white to yellow when heated in air and reverting to white on cooling. This color change is caused by a small loss of oxygen to the environment at high temperatures to form the non-stoichiometric Zn_{1+xO}, where at 800 °C, x = 0.00007. ZnO is used in many products and materials, including cosmetics, food supplements, rubbers, plastics, ceramics, glass, cement, lubricants, paints, sunscreens, and more. It is nearly insoluble in water, but it will dissolve in most acids, such as hydrochloric acid:

$$ZnO + 2\ HCl \rightarrow ZnCl_2 + H_2O$$

Solid zinc oxide will also dissolve in alkalis to give soluble zincates:

$$ZnO + 2\ NaOH + H_2O \rightarrow Na_2[Zn(OH)_4]$$

ZnO reacts slowly with fatty acids in oils to produce the corresponding carboxylates, such as oleate or stearate. When mixed with a strong aqueous solution of zinc chloride, ZnO forms cement-like products best described as zinc hydroxy chlorides. This cement was used in dentistry.

ZnO also forms cement-like material when treated with phosphoric acid; related materials are used in dentistry. A major component of zinc

phosphate cement produced by this reaction is hoplite, $Zn_3(PO_4)_2 \cdot 4H_2O$. (14)

ZnO decomposes into zinc vapor and oxygen at around 1975 °C with a standard oxygen pressure. In a carbothermic reaction, heating with carbon converts the oxide into zinc vapor at a much lower temperature (around 950 °C).

$$ZnO + C \rightarrow Zn_{(Vapor)} + CO$$

1.4.1. Structure of ZnO

Zinc oxide crystallizes in two main forms, hexagonal wurtzite and cubic zincblende. The wurtzite structure is most stable at ambient conditions and thus most common. The zincblende form can be stabilized by growing ZnO on substrates with cubic lattice structure. In both cases, the zinc and oxide canters are tetrahedral, the most characteristic geometry for Zn (II). ZnO converts to the rock salt motif at relatively high pressures about 10 G Pa.(15)

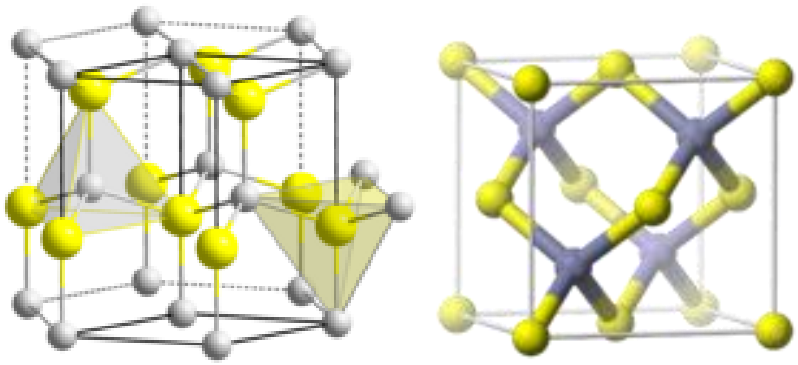

***Fig 1.5 Wurtzite structure and zincblende unit cell of ZnO. Reprinted from reference** (15)*

Hexagonal and zincblende polymorphs have no inversion symmetry (reflection of a crystal relative to any given point does not transform it into itself). This and other lattice symmetry properties result in piezoelectricity of the hexagonal and zincblende ZnO, and pyroelectricity of hexagonal ZnO.

The hexagonal structure has a point group 6 mm (Hermann–Mauguin notation) or C_{6v} (Schoenflies notation), and the space group is $P6_3mc$ or C_{6v}^4. The lattice constants are a = 3.25 Å and c = 5.2 Å; their ratio c/a ~ 1.60 is close to the ideal value for hexagonal cell c/a = 1.633. As in most group II-VI materials, the bonding in ZnO is largely ionic ($Zn^{2+}O^{2-}$) with the corresponding radii of 0.074 nm for Zn^{2+} and 0.140 nm for O^{2-}.

1.4.2. Mechanical properties

ZnO is a wide-band gap semiconductor of the II-VI semiconductor group. The native doping of the semiconductor due to oxygen vacancies or zinc interstitials is n-type. ZnO is a relatively soft material with approximate hardness of 4.5 on the Mohs scale. Its elastic constants are smaller than those of relevant III-V semiconductors, such as GaN. The high heat capacity and heat conductivity, low thermal expansion and high melting temperature of ZnO are beneficial for ceramics. The E2 optical phonon in ZnO exhibits an unusually long lifetime of 133 ps at 10 K. (16)

Among the tetrahedrally bonded semiconductors, it has been stated that ZnO has the highest piezoelectric tensor, or at least one comparable to that of GaN and AlN. This property makes it a technologically important material for many piezoelectrical applications, which require a large electromechanical coupling. Therefore, ZnO in the form of thin film has

been one of the most studied and used resonator materials for thin-film bulk acoustic resonators.

1.4.3. Electrical and optical properties

Favourable properties of zinc oxide include good transparency, high electron mobility, wide band gap, and strong room-temperature luminescence. Those properties make ZnO valuable for a variety of emerging applications: transparent electrodes in liquid crystal displays, energy-saving or heat-protecting windows, and electronics as thin-film transistors and light-emitting diodes. ZnO has a relatively wide direct band gap of ~3.3 eV at room temperature. Advantages associated with a wide band gap include higher breakdown voltages, ability to sustain large electric fields, lower electronic noise, and high-temperature and high-power operation. The band gap of ZnO can further be tuned to ~3–4 eV by its alloying with magnesium oxide or cadmium oxide. Due to this large band gap, there have been efforts to create visibly transparent solar cells utilising ZnO as a light absorbing layer. However, these solar cells have so far proven highly inefficient.

Most ZnO has *n*-type character, even in the absence of intentional doping. Nonstoichiometric is typically the origin of n-type character, but the subject remains controversial. An alternative explanation has been proposed, based on theoretical calculations, that unintentional substitutional hydrogen impurities are responsible. Controllable n-type doping is easily achieved by substituting Zn with group-III elements such as Al, Ga, In or by substituting oxygen with group-VII elements chlorine or iodine. Reliable p-type doping of ZnO remains difficult. This problem originates from low solubility of p-type dopants

and their compensation by abundant n-type impurities. This problem is observed with GaN and ZnSe. Measurement of p-type in "intrinsically" n-type material is complicated by the inhomogeneity of samples.(16)

Current limitations to p-doping limit electronic and optoelectronic applications of ZnO, which usually require junctions of n-type and p-type material. Known p-type dopants include group-I elements Li, Na, K; group-V elements N, P and As; as well as copper and silver. However, many of these form deep acceptors and do not produce significant p-type conduction at room temperature. Electron mobility of ZnO strongly varies with temperature and has a maximum of ~2000 $cm^2/(V \cdot s)$ at 80 K. Data on hole mobility are scarce with values in the range 5–30 $cm^2/(V \cdot s)$. ZnO discs, acting as a varistor, are the active material in most surge arresters. Zinc oxide is noted for its strongly nonlinear optical properties, especially in bulk. The nonlinearity of ZnO nanoparticles can be fine-tuned according to their size. Zinc oxide (ZnO) photocatalytic degradation is a process that uses UV light to break down pollutants in water and air:

1.4.4. The Mechanism of ZnO photocatalysis

When ZnO is exposed to UV light, electrons in the valence band move to the conduction band, creating electron-hole pairs. These pairs migrate to the ZnO surface and participate in redox reactions. The holes oxidize dyes or react with water to create hydroxyl radicals, while the electrons reduce oxygen to create superoxide radicals. These radicals attack pollutants on the ZnO surface.(17)

ZnO can be used to treat wastewater, purify air, and more. For example, ZnO-based nanomaterials have been used to degrade drugs like

chloramphenicol, paracetamol, spiramycin, ofloxacin, metronidazole, and tetracycline hydrochloride.

- **Factors that affect photocatalytic degradation**

  The photocatalytic activity of ZnO can be affected by:

  - **Doping**: Adding sulphur to ZnO nanoparticles can improve their photocatalytic properties.
  - **Surface area**: A larger surface area can expose more active sites.
  - **Light harvesting**: A stronger light harvesting ability can improve the efficiency of light utilization.
  - **Oxygen vacancies**: Creating oxygen vacancies in ZnO can increase the rate of photocatalytic degradation.

1.4.5. Limitations of Zno photocatalysis-

The primary limitations of a ZnO photocatalyst are its inability to absorb visible light due to its wide band gap, leading to only UV light activation, and the rapid recombination of photogenerated electron-hole pairs, significantly reducing its overall photocatalytic efficiency; this limits its practical applications as most sunlight consists of visible light, not UV light.

- Limited light absorption: ZnO only absorbs UV light due to its wide band gap (around 3.37 eV), which only constitutes a small portion of the solar spectrum, restricting its photocatalytic activity under sunlight.

- Fast electron-hole recombination: Once excited by light, the generated electrons and holes in ZnO quickly recombine, limiting the number of available charge carriers for redox reactions.

- Stability concerns: Depending on the environment, ZnO can be susceptible to dissolution in acidic conditions or photocorrosion in alkaline solutions, affecting its long-term stability.

- Agglomeration tendency: ZnO nanoparticles can tend to clump together, reducing their surface area available for photocatalytic reactions.

Strategies to overcome these limitations:

- Doping with other elements: Adding dopants to the ZnO lattice can modify its band gap, enabling visible light absorption and slowing down electron-hole recombination.

- Heterojunction formation: Coupling ZnO with other semiconductors can facilitate charge separation by creating a built-in electric field at the interface.

- Surface modification: Modifying the surface of ZnO with other materials can improve its stability and prevent agglomeration.

1.4.6. Methods to enhance ZnO photocatalysis-

To enhance ZnO photocatalysis using 2D composite formation, common methods include: coupling ZnO with other 2D materials like graphene oxide (GO), transition metal dichalcogenides (TMDs) like MoS_2, or layered double hydroxides (LDHs) to create heterojunctions, which facilitates efficient charge separation by transferring photogenerated electrons from ZnO to the 2D material, thus minimizing recombination; optimizing the loading amount of the 2D material to achieve the best charge separation; and tailoring the morphology and interface properties of the composite to maximize light absorption and active sites on the surface.

Key points about using 2D composites for enhanced ZnO photocatalysis:

Charge carrier separation: The primary benefit of a 2D composite is its ability to efficiently separate photogenerated electrons and holes due to the built-in electric field at the interface between the ZnO and the 2D material, leading to improved photocatalytic activity.

Increased surface area: Many 2D materials have a large surface area, providing more active sites for the adsorption of reactants and enhancing the overall reaction rate.

Bandgap engineering: By selecting a 2D material with a suitable bandgap, it's possible to tune the band alignment of the composite to optimize light absorption and charge transfer.

Examples of 2D materials used with ZnO for photocatalysis:

Graphene: Due to its high electrical conductivity and large surface area, graphene is often used to improve charge carrier separation in ZnO-based photocatalysts.

Molybdenum sulphide (MoS_2): This transition metal dichalcogenide can form a type-II heterojunction with ZnO, enabling efficient electron transfer.

Graphitic carbon nitride: g-C_3N_4 is another 2D material that can be combined with ZnO to enhance visible light absorption and photocatalytic activity.

MXenes: These 2D materials with excellent electrical conductivity can act as electron sinks, further improving charge separation in ZnO composites.

Synthesis methods for 2D ZnO composites:

Hydrothermal synthesis: A common method to fabricate 2D ZnO composites by mixing ZnO precursors with the 2D material in a hydrothermal environment.

Sol-gel method: This method allows for precise control of the composition and morphology of the composite by mixing the precursors in a solution and then undergoing a sol-gel transition.

Chemical vapor deposition (CVD): CVD can be used to grow 2D materials directly onto ZnO substrates, creating well-defined interfaces.

1.5 MXenes – THE NEW FAMILY OF 2D-NANOMATERIALS

Two-dimensional materials such as graphene, boron nitride nanosheets (BNNC), and transitional metal dichalcogenides (TMDC) are reshaping the landscape of materials science, ushering in a new era of technological advancements. These materials possess unique attributes including exceptional mechanical strength, remarkable flexibility, excellent biocompatibility, and outstanding optical and electrical properties, making them ideal for a diverse range of applications across fields like photoelectronics, drug delivery, energy storage, biotechnology, and thermoelectronics. As scientists delve deeper into exploring the potential of these two-dimensional marvels, we anticipate witnessing groundbreaking progress that will redefine the boundaries of science and technology.(18)

MXene, much like graphene, is a two-dimensional material distinguished by its remarkable properties, including excellent electrical conductivity, a large surface area, exceptional resistance to oxidation, outstanding thermal conductivity, non-toxicity, hydrophilicity, and the ability to easily bond with various species. Additionally, MXene exhibits impressive enzyme immobilization, biocompatibility, high mechanical strength, and remarkable energy storage capabilities. (18)These characteristics make MXene materials highly suitable for a wide range of applications, including electrochemical capacitor sensors, batteries, photocatalysis, electrocatalytic sensors for pollutant detection, water purification, electromagnetic interference shielding, and biomedical devices. The versatility of MXene presents numerous opportunities for innovation and advancement across various industries. Its ability to enhance performance

and efficiency in diverse applications positions it as a promising material for future technological advancements.

MXene materials are comprised of transition metal carbides, nitrides, and carbonitrides, originating from MAX phases, which comprise three constituents. The "M" within the MAX phase signifies transition metals like Sc, Ti, V, Cr, Mn, and Mo. "A" denotes elements found in groups 13 and 14 of the periodic table, such as Al, Si, P, Ga, and Ge. Lastly, "X" represents carbon and nitrogen.

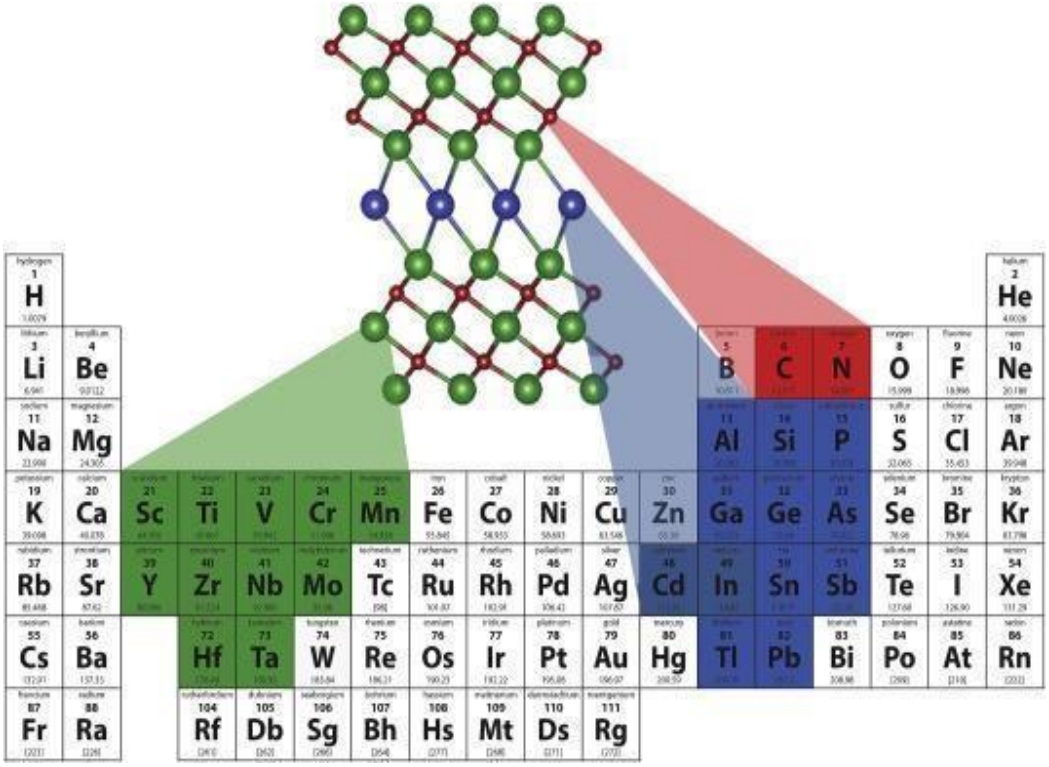

Fig 1.6 Pictorial representation of elements of MAX phase in periodic table. Reprinted from reference *(22).*

The MAX phase, characterized by the general formula $M_{n+1}AX_n$ (where n ranges from 1 to 3), is a three-dimensional material. It is also referred to as a nanolaminated solid due to its layered structure, which imparts a range of notable properties including good thermal conductivity, low hardness, high elastic modulus, excellent oxidation and corrosion resistance, and machinability. MAX phase is further classified into three types or orders denoted by the 211, 312, and 412 unit cells, representing M_2AX, M_3AX_2, and M_4AX_3, respectively.(20)

MXene materials are derived from the exfoliation of MAX Phase compounds, with both MAX Phase and MXene showcasing remarkable properties. The exfoliation process is influenced by the total force constant of the A atom, which is determined by neighboring atoms. As the force constant of A decreases, the exfoliation energy diminishes. Typically, MXene materials have the general formula $M_{n+1}X_nT_x$, where T_x can encompass elements like -O, -F, or -OH, among others. Fabrication of MXene involves etching the A layer from MAX Phase compounds. Common synthesis methods include direct HF etching and indirect in situ HF etching using a mixture of HCl and LiF.Yield is enhanced through delamination processes. (20)

MXene was serendipitously discovered in 2011 by Dr. Yury Gogotsi and Dr. Michel Barsoum, esteemed professors of material science and engineering and fellows of the American Ceramic Society (AcerS) at Drexel University.(21) The initial discovery was $Ti_3C_2T_x$. Future development prospects of MXene and its related advancements within the research sphere are promising. Researchers have pinpointed significant technological applications in supercapacitors, sensors, and photocatalysis. The aim is to provide theoretical guidance and innovative concepts for

synthesizing and developing new and superior MXene materials, ultimately facilitating widespread production and application of this novel material in society.(22)

1.5.1. MXenes: Structure and Type

MXenes are a class of 2D inorganic compounds with Mbenes, consist of thin layer of metal carbides, nitrides or carbonitrides. The Mxene was reported in 2011 in Drexel university, prepared by HF etching from their parent MAX compound. Surface of Mxene are terminated by functional groups, have the general formula $M_{n+1}X_nT_n$, where t is a functional group eg (O, F, OH, CL).(21)

Mono transition: As inherited from the parent MAX PHASES, MXenes adopt three structures, M_2C, M_3C_2, and M_4C_3, with a single metal on the M site. Their usual formula is $M_{n+1}AX_n$, where M is an early transition metal, A is an element from group 13 or 14 of the periodic table, X and/or N, and n = 1–4. They are created by selectively etching out the A element from a MAX phase or other layered precursor (such as Mo_2Ga_2C). With P63/mmc symmetry, MAX phases feature a layered hexagonal structure with X atoms filling octahedral positions and M layers that are almost tightly packed. As a result, the A element, which is metallically bound to the M element, interleaves with the $M_{n+1}X_n$ layers.

Double transition: Metal with a double transition There are two types of MXenes: solid solution MXenes and ordered double transition metal MXenes. The general formulations for ordered double transition metal MXenes are as follows: When M’ and M” are distinct transition metals, the formula is $M'_2M''C_2$ or $M'_2M''_2C_3$. The double transition metal

carbides Mo_2TiC_2, $Mo_2Ti_2C_3$, Cr_2TiC_2, and Mo_4VC_4 have been synthesized. The Mo or Cr atoms on the outside margins of several of these MXenes (such Mo_2TiC_2, $Mo_2Ti_2C_3$, and Cr_2TiC_2) regulate the MXenes' electrochemical characteristics.

In solid-solution MXenes, the metals are dispersed randomly throughout the structure, resulting in continuously adjustable characteristics. Their general formulas are $(M'_{2-y}M''_y)$ C, $(M'_{3-y}M''_y)C_2$, $(M'_{4-y}M''_y)C_3$, or $(M'_{5-y}M''_y)C_4$.

Divacancy: Evidence for 2D Mo1.33C sheets with ordered metal divacancies can be found by selectively etching the Al and Sc atoms and developing a parent 3D atomic laminate, $(Mo_{2/3}Sc_{1/3})_2AlC$, with in-plane chemical ordering.

1.5.2. PROPERTIES OF MXENE

1.5.2.1. ELECTRICAL PROPERTIES

The distinctive 2D layered structure of MXenes contributes significantly to their remarkable and adaptable electrical characteristics. Because of their transition metal atoms, these materials, which are produced from MAX phases, have a high conductivity.(23) These materials are highly conductive and appropriate for a wide range of electronic applications because of the effective charge transport made possible by the transition metal layers inside the MXene structure. MXenes' conductivity is a crucial characteristic that distinguishes them from many other 2D materials, such as graphene or transition metal dichalcogenides, and gives them an advantage in a number of technical fields.

Tunability is a significant feature of MXenes' electrical characteristics. Surface functionalization, which usually involves termination groups like -O, -OH, and -F, can change the electrical structure of MXenes. They can control their electronic band structure, especially the bandgap, thanks to this tunability. The degree and kind of surface termination can determine whether MXenes behave in a metallic or semiconducting manner. This ability to modify the electronic properties through functional groups presents a great deal of promise for creating MXenes with customized electronic properties for certain uses.

Additionally, MXenes have a high charge carrier mobility, which is critical for high-performance electronic device applications. These materials' layered structure permits free electron mobility and smooth charge transfer due to weak interlayer interactions. MXenes are desirable for use in transistors, sensors, and supercapacitors due to their effective electrical conductivity. They are especially good candidates for energy storage devices like batteries and supercapacitors, where quick charge-discharge cycles are necessary, because to their high electronic conductivity and ion intercalation capability.(24)

Furthermore, depending on their chemical composition, MXenes display a broad variety of electrical behavior. It is possible to drastically change their electrical characteristics by changing the transition metal or the amount of carbon or nitrogen. For example, some MXenes behave like semiconductors, while others stay metallic. MXenes' compositional versatility is another feature that makes them very appealing for application in electrical and optoelectronic systems of the future. These materials can be engineered for particular conductivity or

semiconductivity, which increases their use in photodetectors, flexible electronics, and transparent conductive films.

1.5.2.2. THERMAL PROPERTIES

MXene such as Ti_3AlC_2 shows high thermal conductivity and thermal oxidation. $Ti_3C_2F_x$ monolayer has a thermal conductivity of approximately 108 w/mk. In $Ti_3C_2O_x$ monolayers have a thermal conductivity of approximately 11 W/m-K . (25)It is found that, with $Ti_3C_2T_x$ films thermal conductivity is approximately 2.84 W/m-K. The extraordinary flexibility of $Ti_3C_2T_x$ is due to the metallic conductivity at 2400 scm^{-1}. V_2C shows a conductivity of 3300 scm^{-1}.The versatile properties of MXene promise unprecedented applications such as wearable electronics and also in various fields like biomedicine, environmental protection, heat regulation, and sensors. MXene can also use as a photocatalyst and electro-catalyst because of its good conductivity.

1.5.2.3. HYDROPHILICITY PROPERTIES

The hydrophilic nature of MXene is due to the presence of oxygen-containing groups such as O, OH, and F groups in the surfaces. These functional groups make the MXene more attractive to water molecules, resulting in strong interactions and facile wetting. Similar to graphene, MXenes are composed of layers that permit water molecules to intercalate between them. (26)Their hydrophilicity is aided by this characteristic, which intensifies their interaction with water. MXenes' 2D structure gives them a large surface area that increases the number of places for interactions with water molecules, thereby enhancing their hydrophilicity.

By understanding the hydrophilic properties researchers manipulate MXenes to unlock more potential applications such as water purification. Because of their potent interactions with water molecules and different pollutants, methylenes can be employed in membranes and filters to eliminate impurities from water. The hydrophilic surface of MXenes enables effective ion transport in aqueous electrolytes, which is beneficial for supercapacitors and batteries. MXenes are promising options for drug delivery systems and biosensors due to their hydrophilicity and biocompatibility. Reactant accessibility is improved by the hydrophilic surfaces of MXenes, which can improve catalytic reactions in aquatic conditions. The hydrophilicity of MXenes is a critical property that significantly contributes to their flexibility and functionality in various innovative applications

1.5.2.4. OPTICAL PROPERTIES

MXene are the novel materials that exhibit strong interaction with light. Which offers diverse application optoelectronic devices and photonic elements. (24)They posses' strong absorption across the electromagnetic spectrum i.e., from the region of ultraviolet to the region of near infrared, which makes MXene for the application of photothermal therapy, photodetection and solar energy harvesting. MXene shows plasmonic behavior.(27)

1.5.2.5. MECHANICAL PROPERTIES

The mechanical properties of MXenes are strongly dependent on their surface finish. O-terminated MXenes are predicted to have very high stiffness, but MXenes terminated by other groups (F and OH) have lower

elastic stiffness than their O-terminated counterparts. This can be related to the different lattice constants of MXenes with different terminations: in general, O-terminated MXenes have smaller lattice parameters than F^- or OH^-terminated MXenes. Compared to bare MXenes, surface-functionalized MXenes have greater flexibility. Using Ti_2C as an example, it is found that functionalization would lower the Young's modulus of Ti_2C, but functionalized Ti_2C can withstand higher stress than bare Ti_2C and even graphene. The surface-terminated bands act as a buffer layer for Ti_2C under tensile deformation, slowing down the collapse of Ti layers and increasing the critical stress value when Ti_2C breaks. (28)

The number of atomic layers of MXene, defined by the chemical formula $M_{n+1}X_n$ as n, also affects the mechanical properties of MXene. It is studied that the elastic constant and Young's moduli of bare MXenes using classical molecular dynamics. They find that among all $Ti_{n+1}C_n$ (n = 1, 2, 3), the thinnest Ti_2C has the highest Young's modulus and the elastic constant of Ti_2C is almost twice that of MoS_2. For functionalized MXene, it shows that as n decreases, the strength and hardness of $M_{n+1}X_nT_x$ gradually increase. Experimentally, it has been found that the mechanical properties of MXenes are improved by the formation of polymers or carbon nanotube composites.

By combining different types of polymers, MXene's flexibility, durability, and tensile and compressive strength can be improved to varying degrees. For example, $Ti_3C_2T_x$ polyvinyl alcohol (PVA) composite has excellent flexibility and high tensile and compressive strength. In particular, the tensile strength of $Ti_3C_2T_x$-PVA composites is about four times higher than that of isolated $Ti_3C_2T_x$. In addition, $Ti_3C_2T_x$-PAM80 and $Ti_3C_2T_x$-UHMWPE81 were reported to have high durability and performance.

1.5.2.6. PHOTOTHERMAL PROPERTIES

The Photothermal properties of MXene make them more suitable for numerous applications including sensing, optoelectronics, and photothermal therapy. These characteristics are due to their composition, structure, and presence of surface termination.(29)

Photothermal therapy is used for cancer treatment which can convert absorbed light into heat to destroy cancer-affected cells. MXenes, mainly titanium such as $Ti_3C_2T_x$ exhibit strong absorption in the visible and near-infrared regions. The surface of MXene having free electrons causes localized surface plasmon resonance (LSPR) which is the reason for strong absorption.(30)

1.5.2.7. BIOCOMPATIBILITY

Biocompatibility is a critical aspect of their application in fields like drug delivery, bioimaging, and biosensing. MXenes exhibit high biocompatibility due to their ability to be functionalized with various groups such as –OH, –O, and –F, which can reduce cytotoxicity and enhance interactions with biological tissues. (31)Surface modifications can further enhance biocompatibility and reduce potential toxic effects, making MXenes safe for in vivo and in vitro applications. However, the extent of their biocompatibility can vary depending on factors like concentration, exposure time, and the specific type of MXene used.

MXenes' large surface area and ability to respond to environmental stimuli (such as pH and reactive oxygen species) make them effective for

controlled drug release. They can carry and release drugs in a targeted manner, responding to specific conditions within the body, which is beneficial for treatments such as cancer therapy. Additionally, MXenes have been integrated into hydrogels, which mimic the mechanical properties of tissues, providing scaffolds for tissue engineering that promote cell growth and tissue regeneration(32)

MXenes have demonstrated significant antimicrobial properties, which can be enhanced through photothermal effects. When exposed to light, MXenes can convert light energy into heat, effectively killing bacteria. This makes them suitable for applications in wound healing and infection control. Their ability to generate reactive oxygen species under light exposure further contributes to their antibacterial activity

MXenes' excellent electrical conductivity and large surface area make them ideal for biosensing applications. They can detect biological molecules with high sensitivity and specificity, which is valuable in diagnostic tools and wearable sensors. Their integration into electrochemical and optical sensors has been explored for detecting various biomarkers, enhancing the accuracy and reliability of diagnostic procedures

In conclusion, MXenes show great promise in biomedical applications due to their tunable biocompatibility, effective drug delivery capabilities, antimicrobial properties, and potential in biosensing technologies. Future research will likely focus on optimizing their biocompatibility and further exploring their multifunctional roles in various medical applications

1.6. MXenes: SYNTHESIS APPROACHES

About 20 different types of MXene are discovered till date. The desirable MXene are selectively synthesized by etching technique. For the preparation of desired MXene the MAX phases are soaked in specified acids disrupting M-A bonds. Acids like HCL, LIF or NH_4HF_2 and salts like NH_3F, KF, LIF or NAF which contain fluorine ions are used as different types of etching agents. A certain corrosion time and full agitation is needed for the above process to take place.(33)

$Ti_3C_2T_X$ is the first synthesized MXene by soaking Ti_3ALC_2 powders in 50% concentrated hydrofluoric acid at room temperatures for about 2 hours. While studying the results obtained in XRD (X-ray diffraction) treatment. The precursor Ti_3ALC_2 showed peaks around 40 degrees Celsius. Soon after the itching process the peak shifted to 10 degrees Celsius. (34)

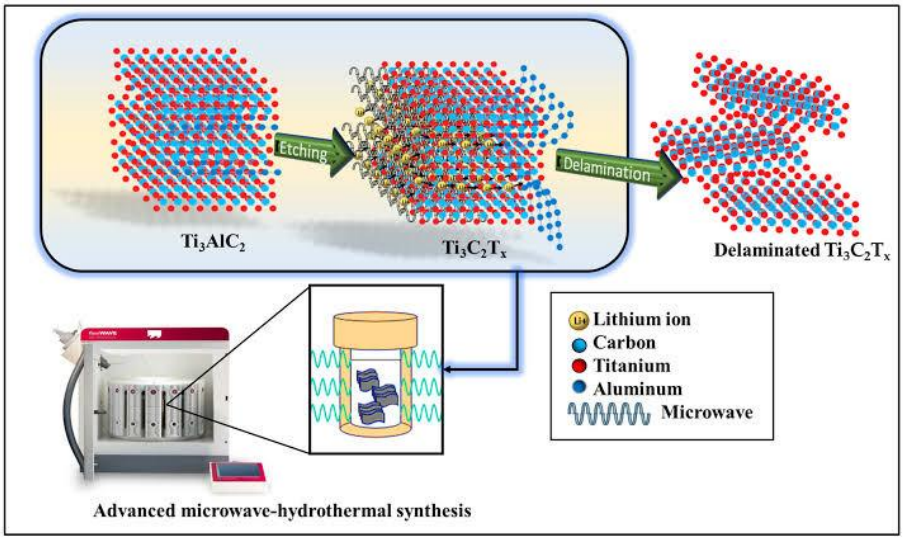

***Fig 1.7 Typical synthesis of MXenes. Reprinted from reference** (38).*

Although HF is very efficient technique used for etching it is very harmful to human body. Alternative etching agents were used for later studies. A mixture of LIF and HCL was found to be useful and was used in the synthesis of MXene. (35)Precursor was soaked in HCL and LIF mixture for 35 minutes for 24 hours to obtain $TI_3C_2T_X$. Thus, synthesized sample show fewer defects as observed from the transmission electron microscopy.(36)

Combinations of H_2SO_4 and fluorine ions like NAF, FEF_3, KF, CSF, CAF_2, could also yield many MXene like TI_2CT_X, MO_2CT_X, V_2CT_X, $TI_3C_2T_X$. Since all of the etching agents have fluorine ions and it produce HF gas. Hilum found an environment friendly etching agent using ammonia and fluorine ions which doesn't liberate HF gas. Fluorine Ions were mixed with ammonium hydroxide producing NH_4HF_2.

The complete conversion of MAX phase into MXene is called the etching process. The essential conditions for etching process vary depending upon the atoms that we take. The chemical formula is denoted as $M_{n+1}AX_n$. When the atomic number of m increases the M-A bond energies increases and the fluorine ion concentration in the etchant solution and etchant ion concentration should be increased. Larger n value requires longer etching time and larger fluorine ion concentration if it becomes less acidic and a higher temperature is required. Therefore, not only acid solution but also salts could be used for the preparation of MXene.

1.6.1. MODIFYING THE STRUCTURE OF MXenes

1.6.1.1. Doping

Doping provides a technique to greatly improve MXenes' functional capabilities. The procedure enables exact control over the characteristics of MXenes, whether metals like cobalt or nickel are added, or non-metals like nitrogen, boron, sulphur, or phosphorus are incorporated. Because of this, they are a very versatile class of materials that may be made to perform particular tasks in a variety of industries, including electronics, energy, and catalysis. MXene doping is a crucial topic of research in the creation of next-generation materials since it keeps opening up new possibilities.(37)

The electrical structure of MXene can be significantly changed by adding elements like phosphorus, nitrogen, sulfur, or boron. By increasing the electrochemical capacitance, nitrogen doping in $Ti_3C_2T_x$ MXene, for instance, has been demonstrated to enhance its performance in supercapacitors. Because nitrogen atoms are smaller and more electronegative than carbon atoms, they affect how electron density is distributed throughout the MXene layers, improving the material's conductivity and capacitance retention.(38) Researchers can optimise MXenes' energy storage properties through this doping procedure, which makes them extremely effective electrode materials. To increase the catalytic activity of MXenes, boron has been added, which is another kind of doping. Compared to their undoped counterparts, boron-doped $Ti_3C_2T_x$ MXenes shown increased hydrogen evolution reaction (HER) activity in one investigation. By adding more active sites to the surface of MXenes, boron atoms enable more effective catalytic reactions. Because of their

enhanced catalytic capabilities, boron-doped MXenes are appealing for application in energy conversion technologies including fuel cells and water splitting. Another tactic that has been investigated to alter the characteristics of MXenes is phosphorus doping. Because phosphorus atoms are bigger than carbon or nitrogen atoms, they can cause structural strain in the MXene layers. The mechanical and electrical characteristics of the material may alter as a result of this strain, which makes phosphorus-doped MXenes appropriate for application in flexible electronic devices and sensors. Furthermore, it has been discovered that phosphorus doping increases MXenes' thermal stability, which is advantageous for applications in challenging conditions. Sulphur doping in MXenes has shown encouraging outcomes for enhancing lithium-sulfur batteries. In lithium-sulfur battery technology, sulphur doping improves the anchoring of polysulfides within the MXene structure, minimising their dissolution into the electrolyte. The inclusion of sulphur atoms strengthens the bond between the polysulfides and MXene layers, improving cycling stability and increasing battery energy densities. Doping MXenes offers many advantages, one of which is the controllable surface chemistry. Depending on the intended use, doping can alter the surface functional groups to increase hydrophilicity or hydrophobicity, such as -OH, -O, and -F. For instance, it has been investigated to dope MXenes with fluorine to improve their hydrophobicity, which may be effective in creating membranes or coatings that are resistant to water. But oxygen doping can increase hydrophilicity, which makes MXenes better suited for aquatic settings like water purification or desalination systems. Doping can also increase MXenes' stability in many chemical conditions.

1.6.1.2. Nanohybrids and Nano composites

MXene based nanocomposites are advanced materials that integrate MXene with other compounds such as polymers, metals or ceramics which leverage their properties that makes them in various applications.(39)

There are different types of MXene nanocomposites.

Polymer nanocomposites:- The MXene embedded into polymers matrics which enhances the electrical, mechanical and thermal properties. They are used in flexible electronics, electromagnetic interface (EMI) shielding, and smart materials.

Metal MXene nanocomposites:- MXene is combined with metals or metal nanoparticles thus increases their catalytic properties mainly making them suitable for photocatalysis, energy conversion and energy storage.

Ceramic MXene nanocomposites:- MXene integrate with ceramics thereby improves its thermal and mechanical stability and making them suitable for high temperature or harsh environmental applications.

Carbon based MXene nanocomposites:- The MXene combined with carbon nanotubes or graphene. Which enhances the electrical and mechanical properties. They are used in batteries, super capacitors and sensors.

1.6.1.3. Formation Techniques of Nanocomposites

The synthesis of nanocomposites involves various methods, depending on the type of matrix and nanofillers used. The primary techniques include:

1. Solution Mixing

This method involves dispersing nanoparticles in a solvent along with the matrix material, followed by solvent evaporation to form a uniform nanocomposite. It is commonly used for polymer-based nanocomposites due to its ability to achieve good dispersion of nanofillers.

2. In Situ Polymerization

In this approach, nanoparticles are introduced into a monomer solution, and polymerization is initiated. This method ensures strong interfacial bonding between the nanofiller and the polymer matrix, leading to improved mechanical and thermal properties.

3. Melt Mixing

A widely used technique in the plastics industry, melt mixing involves blending nanoparticles with a molten polymer using extrusion or injection molding. It is advantageous because it avoids solvent-related environmental concerns and enables large-scale production.

4. Sol-Gel Processing

This method is primarily used for ceramic and hybrid nanocomposites. It involves the hydrolysis and condensation of metal alkoxides, forming a

gel-like network that incorporates nanoparticles. The material is then heat-treated to obtain the final structure.

5. Mechanical Milling

Used for metal-based nanocomposites, this method involves high-energy ball milling, where nanoparticles are dispersed into a metal matrix through mechanical forces. It is effective in producing uniform dispersion but may introduce defects into the material.

1.6.1.1. Properties and Advantages of Nanocomposites

Nanocomposites exhibit superior properties compared to traditional composites due to the high surface area and aspect ratio of nanofillers. Some key advantages include:

Enhanced Mechanical Strength: The addition of nanoparticles significantly improves tensile strength, toughness, and impact resistance.

Improved Thermal Stability: Many nanocomposites exhibit higher heat resistance, making them suitable for high-temperature applications.(40)

Superior Electrical Conductivity: Carbon-based nanofillers, such as graphene and carbon nanotubes, enhance electrical properties, making nanocomposites ideal for electronic applications

Lightweight Nature: Despite their improved properties, nanocomposites maintain a low density, making them ideal for automotive and aerospace industries.

Barrier Properties: Nanoparticles can reduce the permeability of gases and liquids, which is particularly beneficial for food packaging and coatings

Aerospace and Automotive: Used in lightweight structural components, fuel-efficient vehicles, and durable coatings.

Electronics: Applied in flexible circuits, sensors, and electromagnetic shielding materials.

Biomedical Field: Utilized in drug delivery systems, bone implants, and antibacterial coatings.

Energy Sector: Integrated into battery electrodes, fuel cells, and solar panels to enhance performance.(41)

Packaging Industry: Provides improved barrier properties for food and pharmaceutical packaging, extending shelf life.

1.6.2. MXene based nanomaterials for photocatalyst

For the past few year, the photocatalyst was effectively synthesize from the nanocomposites. MXene have been regarded as promising research materials that bearing versatile properties are suitable for the preparation of photocatalyst. There are different methods including hydrothermal treatment, mechanical/ ultrasonic mixing, calculation and electrostatic assembly used for MXene based photo catalysts.(42)

The simplest method for preparing MXene based photocatalyst by mechanical/ ultrasonic mixing. In this process high power ultrasonic

vibration or strong mechanical stirring is used which keep intimate contact between MXene and photocatalyst. For instance, Chl/$Ti_3C_2T_X$ is prepared by mixing chlorophyll-a (Chl) and $Ti_3C_2T_X$ and dry it . The highest H_2 yield is exhibited from 2% Chl/$Ti_3C_2T_X$.

For the generation of 0D/2D, 1D/2D, or 2D/2D MXene based photocatalyst electrostatic assembly process is used. In which a electrostatic interactions between semiconductors with positive charges are easy to assemble with MXene with a large number of negative charges. 1D/2D Cds/Ti_3C_2 composite is made by using electrostatic self assembly process. The Cds nanowires were well distributed on the surface of Ti_3C_2 nanosheets by using electrostatic interactions.

1.6.3. MXenes FOR ENVIRONMENTAL REMEDIATION

MXenes are two-dimensional materials bearing fascinating inherent properties such as excellent chemical stability, rich surface chemistry, strong electrical conductivity, large surface-to-value ratios, and a tunable structure. These characteristics of MXenes make it versatile. One of the important applications is that it is used as a catalyst. Pure MXene and MXene-based composite catalysts have recently seen high demand for energy applications. The recent advance in the uses of MXene-based nanomaterials for catalytic transformation including selected electrochemical reactions, hydrogen evolution reaction (HER), methanol oxidation reaction (MOR), dry reforming of methane (DRM), water gas shift (WGS) reaction, CO oxidation and CO_2 electrochemical reduction, Suzuki-Miyaura coupling reaction, sulfur reduction reaction (SRR).

1.6.4. Application of MXenes as Photocatalysts

Photocatalysis finds diverse applications in environmental and related fields. It involves a chemical reaction where a photo-catalytic material absorbs light energy, thereby accelerating specific reactions. This occurs as photons elevate electrons to higher energy levels upon absorption.

Key applications of photocatalysts include environmental remediation, water splitting for hydrogen generation, self-cleaning surfaces, and solar energy conversion. Titanium dioxide (TiO_2), zinc oxide (ZnO), and various metal oxide semiconductors serve as common photoconductors, each offering unique characteristics and applications. In recent times, photocatalytic water treatment has garnered significant attention due to its advantages such as effectiveness under ambient conditions, affordability, and minimal generation of secondary waste, making it a modern and environmentally beneficial technology for water purification.(43)

Discovering the technical enhancements that MXene and MXene-based nanomaterials bring to photocatalytic reactions is highly valuable. MXene has been of great interest in recent years as a catalyst and as a catalyst to improve the photocatalytic environment and energy.

1.6.4.1 Sensors

MXenes have large surface area that posses' excellent conductance property and good biocompatibility. For more than ten years its used as sensors. It has excellent performance as biosensor and gas sensor.in a biosensor the active protein usually loses it bioactivity. When it is in contact with electron surface. For this surface materials are selected and

used to immobilize active proteins but also simultaneously maintain their activity. MXene act as protein immobilizing matrices. It helps to protect active protein molecules but facilitate the direct electron transfer between the enzyme and the electrode yielding a possibility of creating a mediator free biosensor. Ti_3C_2Tx was the first chosen to immobilize hemoglobin in the biosensor (Nafion) Hb/Ti_3C_2Tx/GCE for detecting nitriles. Ti_3C_2Tx have relatively high conductivity, the Nafion Hb/Ti_3C_2Tx GCE biosensor shows an excellent performance with an enlarged detection range and a reaction detection limit.(44)

MXene is not only used in biosensor but also in gas sensor. MXene in gas sensors overcomes conventional gas sensors but it doesn't absorb ammonia. Yu et al was the first to investigate adsorption of gas molecules (NH_3, H_2, CH_4, CO) on monolayer $TiCO_2$. It is seen that NH_3 is adsorbed on $TiCO_2$ shows large fluctuation in contrast to weak fluctuation of the corresponding curves of MoS_2 and phosphorene in some cases. Indicating the high sensitivity of TiO_2 to NH_3. The MXene – Ti_3C_2Tx is fabricating subsequently. This sensor successfully measures various gas (ethanol, methanol, acetone, ammonia) at room temperature and shows p- type sensing behavior Ti_3C_2Tx sensor shows highest affinity to NH_3 and lowest mechanism of the TiC_2T_x sensor involves adsorption desorption of gases by both defects and function groups of $Ti_3C_2T_x$.(45)

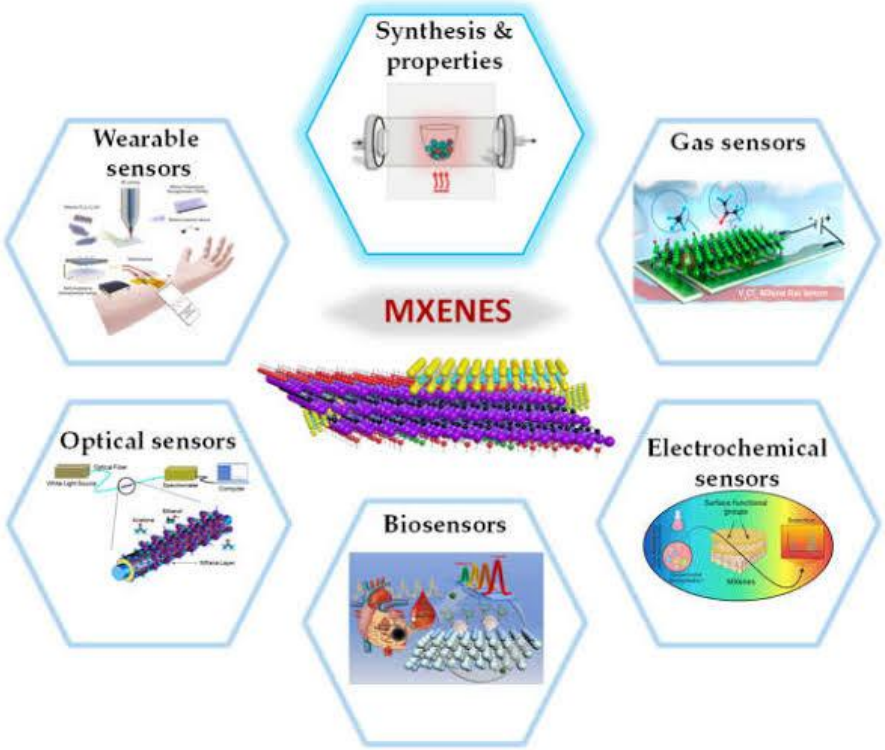

***Fig 1.8 Properties of MXene. Reprinted from reference** (49).*

1.6.4.2. Dye adsorption

The use of dye and effective removal from bodies have to be efficiently. Therefore, an effective and environment friendly technique is to be used. 2D transmission metal carbides or nitrides of MXene have excellent physiochemical property. So, they have large surface area variable surface chemistry and superior adsorption capability. Several properties of MXene were studied special adsorption process for dye removal. Thorough analysis of effects of several variables including dye concentration and temperature on the adsorption efficiency of MXene was performed. MXene can be used as adsorbents and portrays them as promising and long-lasting adsorbents for the removal of synthetic dyes from water.

1.7 POLYCAPROLACTUM (PCL) FOR WATER TREATMENT APPLICATIONS

Polycaprolactone (PCL) is a synthetic, semi-crystalline, biodegradable polyester with many properties, including:

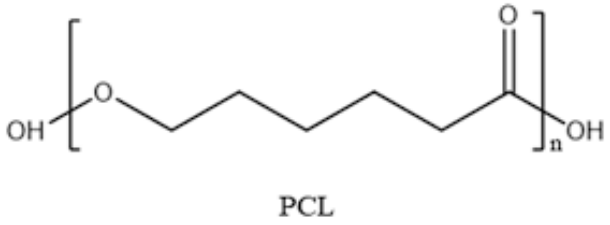

PCL

Fig 1.9 Structure of PCL*. Reprinted from reference (16).*

- **Chemical properties**: PCL is a polyester compound that can be modified by changing its chemical structure and degree of crystallinity.
- **Mechanical properties**: PCL has attractive mechanical properties that make it suitable for a wide range of uses.
- **Biocompatibility**: PCL is biocompatible and can be used in biomedical applications such as sutures and drug delivery devices.
- **Solubility**: PCL is soluble in many different organic solvents.
- **Degradation**: PCL can be degraded without polluting the environment by hydrolysis of ester bonds and microorganisms. However, PCL has a long degradation time.

- **Compatibility**: PCL is compatible with several other polymers.

- PCL is a semi-crystalline polymer with a chemical formula of [-OC(O)C6H10-]n, where n represents the number of monomer units in the polymer chain. The caprolactone monomers are connected through ester bonds between the carboxyl (-COOH) group of one monomer and the hydroxyl (-OH) group of another.

- **Electrical properties**

  PCL has low conductivity. However, the conductivity of the overall solution can be increased by adding low-polarity molecules to the spinning solution. (48)

  PCL is a synthetic, semi-crystalline, biodegradable polyester with a melting point of about 60 °C and a glass transition temperature of about −60 °C. The most common use of polycaprolactone is in the production of specialty polyurethanes. Polycaprolactones impart good resistance to water, oil, solvent and chlorine to the polyurethane produced.

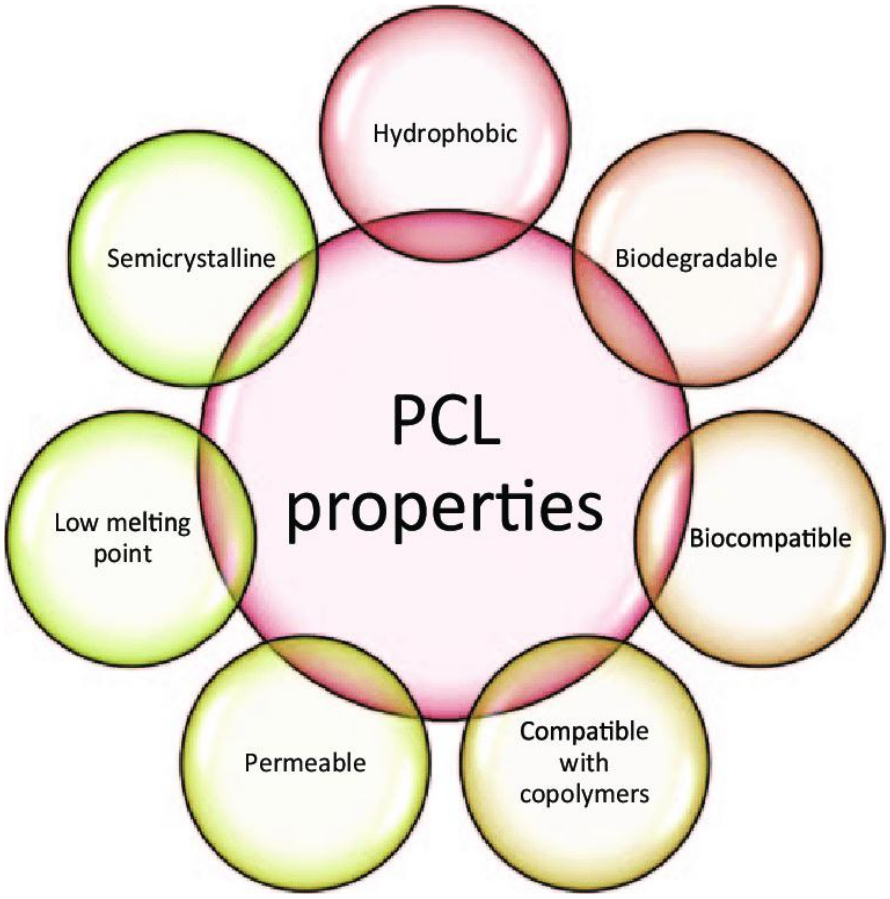

***Fig 1.10 Properties of PCL. Reprinted from reference** (49)*

- This polymer is often used as an additive for resins to improve their processing characteristics and their end use properties (e.g., impact resistance). Being compatible with a range of other materials, PCL can be mixed with starch to lower its cost and increase biodegradability or it can be added as a polymeric plasticizer to polyvinyl chloride (PVC).

- Polycaprolactone is also used for splinting, modeling, and as a feedstock for prototyping systems such as fused filament fabrication 3D printers.

***Fig 1.11 PCL beads. Reprinted from reference** (19).*

PCL is biodegradable. *Bacillota* and *Pseudomonadota* can degrade PCL. *Penicillium* sp. strain 26-1 can degrade high density PCL; though not as quickly as thermotolerant *Aspergillus* sp. strain ST-01. Species of *Clostridium* can degrade PCL under anaerobic conditions.(50)

PCL is a hydrophobic, biodegradable, aliphatic polyester. It has a low glass transition temperature and low melting point, and is highly soluble. PCL is also biocompatible and non-toxic. (51)

PCL is used in a variety of applications, including:

- **Biomedicine**: PCL is used in tissue engineering and drug delivery.
- **Food packaging**: PCL is used in food packaging.

- **Blends**: PCL is a good component for blends because of its stability, miscibility, and hydrophobicity.

- **Implantable contraceptives**: PCL's release characteristics have been investigated for use as an implantable contraceptive.

Chapter 2

Literature Survey

Studies on MXenes has expanded significantly since their discovery in 2011 at Drexel University by Gogosti and Anasori (55), highlighting their unique properties and diverse applications. MXenes are two-dimensional materials composed of early transition metals interleaved with carbon or nitrogen, following the formula $M_{n+1}\ X_n\ T_x$, where T_x represents various surface terminations such as O, OH, F, and Cl. Initially, the synthesis of MXenes relied on fluoride-containing compounds, which posed safety and scalability challenges. However, recent advancements have introduced fluoride-free synthesis methods, such as using molten $ZnCl_2$, broadening the accessibility of MXenes for research and application. The applications of MXenes are varied, with significant exploration in energy storage, biomedical fields, and electromagnetic interference shielding. The first major application was in energy storage, but biomedical applications, including photothermal therapy and biosensors, have rapidly gained traction, indicating a shift in research focus. The field has witnessed remarkable growth, with over 750 research institutions from 50 countries contributing to the literature, resulting in the synthesis of more than 30 different MXene compositions. The organization of international conferences, such as the 2nd International Conference on MXenes in 2019, underscores the expanding community and interest in this area, covering a wide range of topics from basic science to practical applications. Overall, the literature on MXenes reflects a dynamic and evolving field, marked by

advancements in synthesis methods, a broadening scope of applications, and a growing global research community.

Research on photocatalytic water purification highlights the challenges posed by wastewater generated from a range of sources, including domestic and commercial operations, as well as the increasing need for clean water globally. In order to lessen environmental contamination and the risks that waterborne infections bring to public health, this wastewater must be treated efficiently. Using active oxidation processes to convert harmful compounds into harmless inorganic molecules like CO_2 and H_2O, photocatalysis is a promising method for decomposing persistent organic pollutants. Titanium dioxide (TiO_2) stands out among the other photocatalysts because of its affordability, non-toxicity, and reusability. However, the main drawback of this technology is that it requires UV light to activate, which limits its effectiveness in visible light. In order to tackle this issue, scientists have investigated chemical alterations such doping TiO_2 with transition metals and forming heterojunctions using non-metallic carbon-based substances like graphitic carbon nitride (g-C_3N_4). Through improved charge separation and bandgap narrowing, these changes seek to increase photocatalytic activity. TiO_2/g-C_3N_4 nanohybrid production has become popular, and a number of approaches, such as pyrolysis and sol-gel procedures, have been used. Improved photocatalytic activity has been demonstrated by these hybrids, especially in the breakdown of dyes and other organic contaminants. Since it reduces secondary pollution from dispersed photocatalysts by combining photocatalytic processes with physical separation, the integration of photocatalysts into membrane systems has also been investigated. TiO_2/g-C_3N_4 hybrids have been shown to be successful in electrospun membranes

in recent investigations, indicating their potential for scalable wastewater treatment applications. Water filtration systems can effectively employ these membranes since they not only improve pollutant degradation but also show outstanding stability over several cycles. The literature emphasizes the importance of creating effective photocatalytic materials and systems in order to address the urgent problem of water pollution on a worldwide scale. (52)

Chapter 3

Materials and Method

3.1 INTRODUCTION

This chapter includes the characterization techniques, materials, and methods used for the synthesis and characterization of ZnO, MXene ZnO/MXene and preparation of electrospun membrance with PCL, PCL/MXene, PCL/ZMX.

3.2 SYNTHESIS OF ZnO NANOPARTICLES

3.2.1 CHEMICAL AND INSTRUMENTS

Chemical required

- Cetyltrimethylammonium bromide (CTAB) – 0.025 g
- 1% acetic acid – 50 mL
- $ZnAc_2.2H_2O$ – 0.439g
- NaOH – 2 g

Apparatus required

- Autoclave
- Hot air oven
- Filter apparatus
- Glass rod
- Beaker
- Measuring flask
- Weighing machine

3.2.2 PROCEDURE

Take 0.025g of cetyltrimethyl ammonium bromide and to this add 1% glacial acetic acid. 1% glacial acetic acid is prepared by adding 49.5 ml distilled water and 0.5 ml of glacial acetic. To the 1% 50ml glacial acetic acid with 0.025g of cetyltrimethyl ammonium bromide add 10mM $ZnAc_2.2H_2O$. 10mM $ZnAc_2.2H_2O$ is prepared by adding taking 0.439g of $ZnAc_2$.2H2o in 50ml distilled water. 1% 50ml glacial acetic acid with 0.025g of cetyltrimethyl ammonium bromide add 40mM $ZnAl_2.2H_2O$ is stirred for about 16 hours.

After stirring for 16 hours 2 ml 10 mM NaOH solution is added dropwise. The NaOH solution is prepared by taking 2g NaOH pellets and dissolve in 5 ml water by using ultrasonicator. Ph of the solution will be almost around 11 and is stirred for 30 minutes. Further 50ml of the above solution is taken and kept in a hydrothermal autoclave at 100° C for about 6 hours and is filtered. Thereby pure ZnO is this obtained.

3.3 SYNTHESIS OF 10% ZMX

3.3.1 CHEMICAL AND INSTRUMENTS

Chemical required

- MXene – 3.2ml
- Cetyl trimethylammonium bromide (CTAB) – 0.025 g
- 1% acetic acid – 50 mL
- $ZnAc_2.2H_2O$ – 0.439g
- NaOH – 2 g

Apparatus required

- Autoclave
- Hot air oven
- Filter apparatus
- glass rod
- beaker
- measuring flask

Fig 3.1. Autoclave used for the synthesis

3.3.2 PROCEDURE

Take 0.025g of cetyl trimethyl ammonium bromide and to this add 1% glacial acetic acid .1% glacial acetic acid is prepared by adding 49.5 ml distilled water and 0.5 ml of glacial acetic .To the 1% 50ml glacial acetic acid with 0.025g of cetyl trimethyl ammonium bromide add 10mM $ZnAc_2.2H_2O$. 10mM $ZnAc_2.2H_2O$ is prepared by adding taking 0.439g of

$ZnAc_2.2H_2O$ in 50ml distilled water. Mxene solution is well mixed by using ultrasonicator from this 3.2 ml is added to the above solution. It is stirred for about 16 hours.

After stirring for 16 hours 2 ml 10mM NaOH solution is added dropwise. The NaOH solution is prepared by taking 2g NaOH pellets and dissolve in 5 ml water by using ultrasonicator. PH of the solution will be almost around 11 and is stirred for 30 minutes. Further 50ml of the above solution is taken and kept in a hydrothermal autoclave at 100° C for about 6 hours and is filtered. Thereby pure ZnO is this obtained.

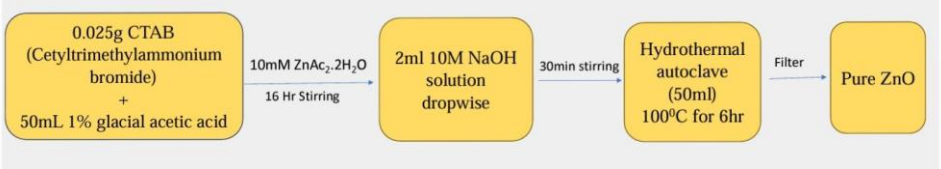

Fig 3.2. Flowchart of synthesis of ZnO.

3.4 PREPARATION OF MEMBRANES BASED ON PCL

3.4.1 CHEMICALS AND INSTRUMENTS

Chemical required

• Methanol – 4.5 ml

• Chloroform – 10.5 ml

• PCL (polycaprolactam) – 2.25 g

Apparatus required

• Electrospinning machine

• Vails

• Measuring flask

• Weighing machine

• Syringe

3.4.2 PROCEDURE

PREPARATION OF POLYMER SOLUTION

Take 4.5 ml methanol and 10.5 ml chloroform and mix it well by placing it on a stirrer. Weigh 2.25 g PCL from this add 2-3 beads to the above solution and dissolve it. This is repeated until the complete addition of PCL beads. Then stir it for 3.5 hours. The polymer solution is obtained. For the fabrication of PCL/MXene and PCL/ZnO-MXene membranes, the required catalyst is added in 5 wt

PREPARATION OF PCL MEMBRANE VIA ELECROSPINNING METHOD

Electrospinning is the fabrication process which works based on electro hydrodynamic principle. This method is used for producing nanofibers. High voltage is required for the fabrication of nanofibers. By this high voltage the liquid droplets becomes charged and the liquid gets stretched due to electrostatic repulsion which counteracts the surface tension. As the jet dries in flight, it get solidified and collected as nanofibers in ground collector.

Following are the parameters adopted:

- Syringe diameter – 15 mm
- Duration – 300 min
- Flowrate – 4 ml/h
- Speed – 500 Rpm
- Duration–300 min

Adjust the distance between the mandrel and syringe about 12 cm. The mandrel is covered the aluminum foil. Then fill the syringe with 8 ml of PCL solution. Apply the voltage about 10 kV/eV. (Check the ground). Start the program first run the mandrel then the syringe . The spinning of polymer solution makes nanofibers. Spin it for 3 hours. The PCL membrane is obtained. It is carefully detached from the mandrel.

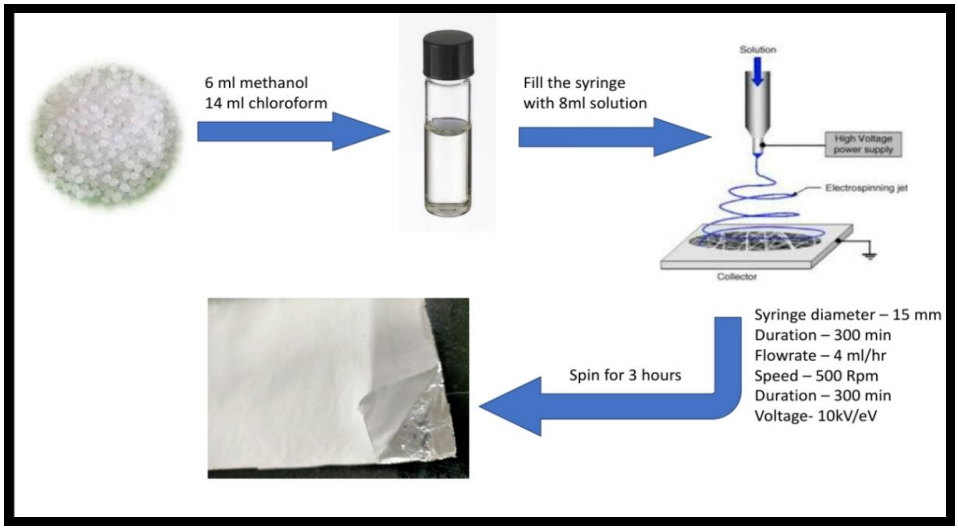

Fig 3.3. Schematic diagram of preparation of PCL Membrane

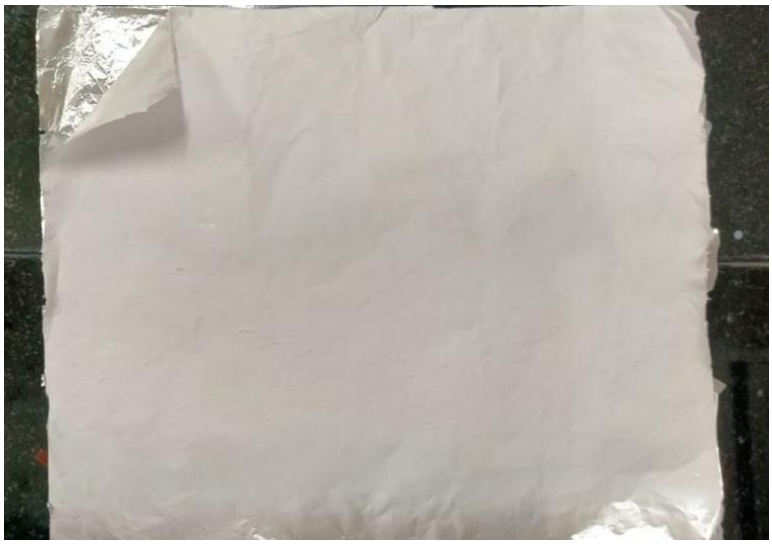

Fig 3.4. The as-spun PCL Membrane using an electrospinning unit.

3.5 PREPARATION OF PCL/MXene MEMBRANE and PCL/ZMX MEMBRANE

3.5.1 CHEMICALS AND INSTRUMENTS

Chemicals required

• Methanol – 4.5 ml

• Chloroform – 10.5 ml

• PCL (polycaprolactam) – 2.25 g

• MXene or ZMX catalyst

Apparatus required

• Electrospinning machine

• Vails

• Measuring flask

• Weighing machine

• Syringe

3.5.2 PROCEDURE

PREPARATION OF POLYMER SOLUTION

Take 4.5 ml methanol and 10.5 ml chloroform and mix it well by placing it on a stirrer. Weigh 2.25 g PCL from this add 2-3 beads to the above solution and dissolve it. This is repeated until the complete addition of PCL beads. Add MXene or ZMX catalyst (5 wt%) to this solution. Then stir it for 3.5 hours. The polymer solution dispersed with the respective catalyst is obtained.

Thereafter the polymer solution is spun in a electrospinning machine undertaking similar parameters and similar procedure as stated in section 3.5.

3.6 WORKING OF ELECTROSPINING UNIT

Electrospinning is an inexpensive and versatile method for the fabrication of ultrafine fibers, generally ranging from the nanometer to micrometer scale. The technique has been drawing considerable attention as it offers the versatility to create continuous fibers with a high surface-area-to-volume ratio, which finds application in the fields of filtration, biomedical applications, drug delivery, and energy storage. The technique is based on the utilization of an electrical field to pull out polymer solutions to form fibers, creating nonwoven mats or aligned fiber architecture.

Electrospinning is regarded as an electrohydrodynamic process, and this is because it depends on the transportation of charged fluid by means of an

electric field. The idea of electrospinning has been present since the early 20th century, but its major application in nanotechnology and material science has increased in the last few decades.(50)

Fig 3.5. Electron Spinning Unit (Holmarc Opto-Mechatronics Ltd, India) used for the fabrication of membranes.

3.6.1 Principle of Electrospinning

The basic concept of electrospinning is attributed to the behavior of electrical forces on polymer liquids. When there is a high voltage applied across a polymer melt or solution, it creates an electric charge over the liquid's surface. With the equilibrium existing between surface tension and

electrostatic repulsion, a conical structure at the liquid surface arises, referred to as the Taylor cone.(50)

At a particular voltage, the electrostatic forces break through the surface tension, and a narrow jet of polymer solution is released from the tip of the cone. The jet is stretched and elongated by electrostatic repulsion at a high rate and forms fibers as the solvent evaporates or the polymer solidifies. The fibers are collected on a grounded or oppositely charged collector, forming a nonwoven fiber network or aligned fibers based on the collection mode.

3.6.2. Electrospinning Mechanism

The electrospinning process occurs in several different stages:

•Charge Induction and Taylor Cone Formation: Charges accumulate on the surface of the liquid when a high voltage is applied to the polymer melt or solution. The liquid takes the form of a Taylor cone as a result of the balance between electrostatic and surface tension forces.

• Jet Initiation and Elongation: With the imposed voltage beyond a critical value, electrostatic forces reach a level where they can overcome the surface tension, and a thin jet of polymer is ejected at the cone tip. The jet initially travels in a straight path but then experiences bending instability, stretching, and thinning.

•Whipping Instability and Solidification: The polymer jet, being electrostatically charged, goes through whipping motion at high frequency, decreasing its diameter even more. The solvent evaporates (in

solution electrospinning) or the polymer solidifies (in melt electrospinning) to form solid fibers.

•Deposition and Collection of Fibers: Fibers deposit on a grounded collector and form a porous, nonwoven mat or aligned fibers depending on the nature of the collector.

3.7 CHARACTERISTION TECHNIQUES

3.7.1. Scanning Electron Microscopy (SEM)

One of the most commonly used techniques in the characterization of nanostructures and nanomaterials is the scanning electron microscope (SEM). Signals produced due to electron-sample interactions give information about the sample, including its chemical composition and surface texture. In a SEM, electrons are accelerated with a large amount of kinetic energy. When the incident electrons are decelerated in a solid specimen, the energy is dissipated as a range of signals produced by the electron-sample interaction. As a result of extremely thin electron beams, SEM micrographs possess a great depth of field providing a three-dimensional look helpful for realizing the surface topology of the sample. When there is an electron beam that approaches and strikes the atoms of the specimen those atoms take their energy and emit their own electron-secondary electron. There is a detector to detect the secondary electron whose charge is positively about 300 V. (51)

Secondary Electrons (SE) are released from just near the surface of the specimen and can be used to get a very high-resolution image of the

sample surface exposing details below 1nm. The electron beam is typically scanned in a raster and the position of the beam is added to the signal that is detected to create an image of the surface. SEM takes more time-consuming sample preparation. The information derived is visual and descriptive, it is not normally quantitative because only a few particles are visible in the field of view at one time.

One of its key benefits is that it can obtain a far deeper depth of field and magnification than optical microscopes, enabling detailed surface analysis on the nanometer scale. SEM can also be integrated with Energy Dispersive Spectroscopy (EDS) to analyze the elemental composition of a sample. This renders it extremely valuable in many disciplines like material science, where it assists in the analysis of metals, polymers, and ceramics; biology and medicine, in the analysis of cell structures and microorganisms; and forensic science, in the analysis of residues and fake materials. It is also extensively used in electronics and nanotechnology to analyze microchips and circuits and in geology to analyze minerals and rock formations. Owing to its flexibility and accuracy, SEM is very important in scientific study and industry use.

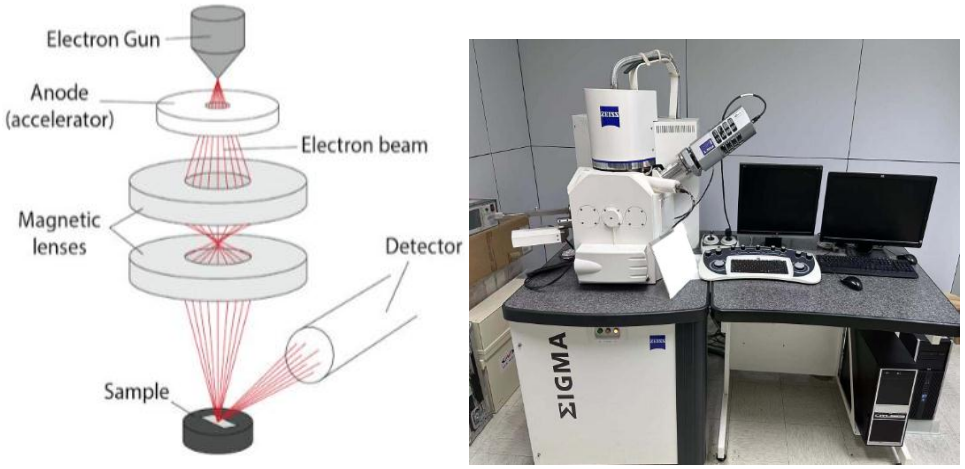

Fig 3.6. Typical diagrammatic sketch explaining the working of SEM, and the SEM instrument (ZEISS Sigma, Germany) used for this study.

3.7.2. X-ray Diffraction (XRD)

XRD is an excellent analytical method that is applied in the identification of the degree of crystallinity or amorphous content, phases present, phase concentrations, structure, and crystallite size and strain are all indicated by the powder diffraction pattern of the nanomaterial. The average size of the crystallites is measured by the widths of the peaks in a particular phase pattern; large crystallites give sharp peaks, and the increase in peak width indicates a smaller crystallite size. structure, composition, and physical characteristics of materials.(52) The underlying concept for XRD revolves around the scattering of X-rays by a crystalline material. When X-ray radiation illuminates a crystal, it becomes diffracted along certain directions following Bragg's Law:$n = 2d\sin\theta$

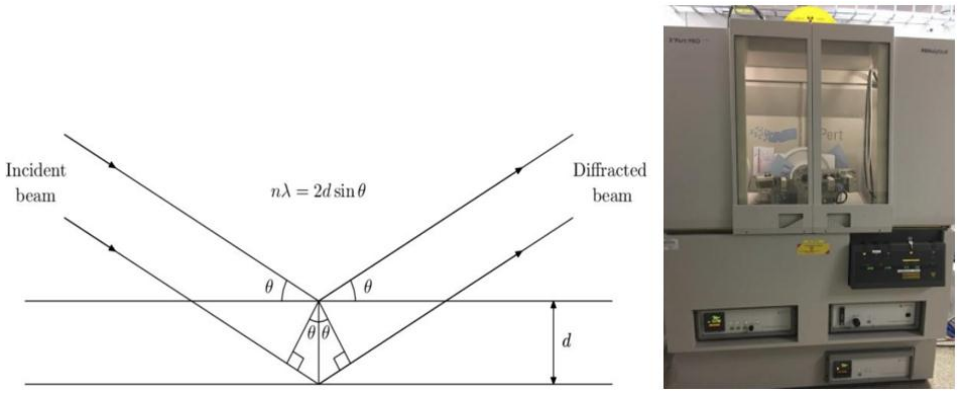

Fig 3.7. Principle of X-ray diffraction, and the X-ray Diffractometer (X'Pert Pro PANalytical) used for this study.

For diffraction to take place, the difference in path between reflected waves from two different crystal planes should be an integer multiple of the wavelength of the X-rays. This causes constructive interference, leading to a diffraction pattern characteristic of the structure of the material. The degree of crystallinity or amorphous content, phases present, phase concentrations, structure, and crystallite size and strain are all indicated by the powder diffraction pattern of the nanomaterial. The average size of the crystallites is measured by the widths of the peaks in a particular phase pattern; large crystallites give sharp peaks, and the increase in peak width indicates a smaller crystallite size.

XRD has extensive applications across different scientific and industrial disciplines. In materials science, it facilitates the identification of crystalline phases, the detection of defects, and the examination of stress-strain effects in metals and ceramics. It also finds applications in geology

for the analysis of minerals, pharmaceuticals for analyzing drug purity and polymorphism, and forensic science for the identification of materials.

3.7.3. RAMAN Spectroscopy

Raman spectroscopy is a strong analytical tool for the interpretation and characterization of materials according to their molecular composition and structure. Through the study of the Raman shift, which is analogous to the vibrational modes of chemical bonds, this method presents a distinctive fingerprint for various materials. It is commonly applied for the identification of chemical identity, crystallinity, phase composition, and molecular interactions in solids, liquids, and gases. Raman spectroscopy relies on the phenomenon of inelastic scattering of light, or Raman scattering. When a monochromatic laser beam is incident on a molecule, the majority of the light is elastically scattered (Rayleigh scattering) without energy change. A small portion of the scattered light experiences an energy shift because of interactions with molecular vibrations. This energy change, known as the Raman shift, is associated with the vibrational modes of the molecule and yields a characteristic spectral fingerprint. Raman scattering is manifested in two modes: Stokes scattering, in which the scattered photon loses energy and the molecule is excited to a higher vibrational state, and Anti-Stokes scattering, in which the scattered photon gains energy from an already excited molecule. Through the examination of these changes, Raman spectroscopy facilitates identification and determination of molecular structures, chemical compositions, and material properties.(53)

Every material has a specific set of vibrational modes that come as discrete peaks in a Raman spectrum. These peaks are useful for identifying chemical compounds, discriminating between polymorphs, and identifying impurities. For instance, graphene and carbon nanotubes possess unique Raman signatures that indicate their structural purity and integrity.

Raman spectroscopy is able to differentiate between two different crystalline and amorphous phases of a material. For example, in semiconductors such as silicon, the position and sharpness of the Raman peak reflect the crystallinity level. Materials undergo stress and strain during production or application, which can cause the Raman peaks to shift due to variations in bond vibrations. In semiconductor devices, coatings, and composites, Raman spectroscopy is employed to measure mechanical stress, which enhances material durability and performance. In nanotechnology, Raman spectroscopy is critical for the analysis of graphene, carbon nanotubes, and quantum dots. It gives information on layer thickness, defects, and electronic properties. Thin films employed in solar cells and optical coatings can also be analyzed for uniformity and composition. Raman spectroscopy is very sensitive to impurities, defects, and chemical contaminants in materials. This is critical in such sectors as pharmaceuticals, food safety, and forensic science, where it is imperative to identify trace amounts of undesired substances to assure quality control.

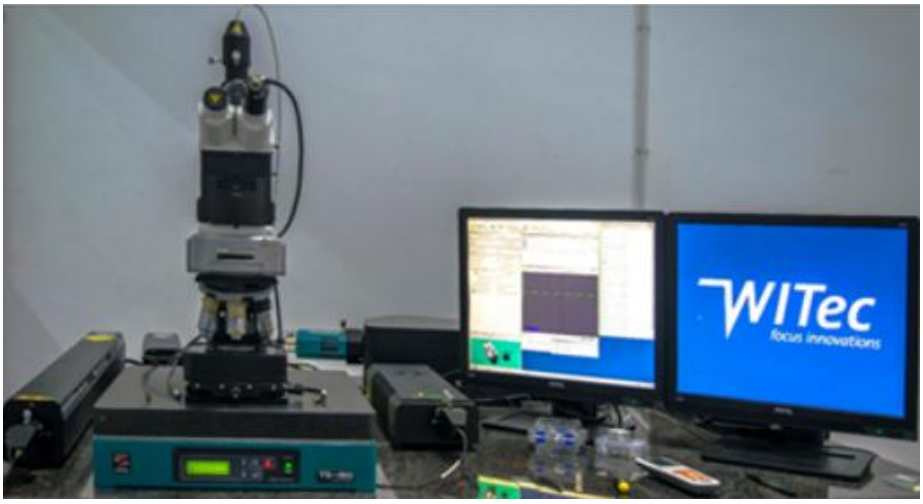

Fig 3.8. The confocal Raman Microscope (WITEC ALPHA300 RA, Germany) used for this study.

3.7.4 UV-Visible spectroscopy

UV-Visible spectroscopy is a sensitive analytical method applied to investigate the electronic structure of molecules through examination of their UV and visible light absorption. It relies on the fact that when molecules are irradiated with UV light, electrons in atoms or bonds within them absorb energy and move from a lower to a higher electronic state. The most frequent transitions found in organic molecules are $\pi \rightarrow \pi^*$, $n \rightarrow \pi^*$, and $\sigma \rightarrow \sigma^*$ transitions, which take place in conjugated systems, molecules with lone pairs, and plain covalent bonds, respectively. The pattern of absorption is important information regarding the molecular structure, functional groups, and conjugation of a compound.(54)

One of the fundamental principles that regulate UV-Vis spectroscopy is the Beer-Lambert law, which is a principle that dictates that the absorbance of a molecule is proportional to its concentration and sample

path length. This makes quantitative analysis possible, and thus UV-Vis spectroscopy can be applied in determining the concentration of unknown compounds. The presence of chromophores—molecular groups that absorb light, including carbonyls, alkenes, and aromatic rings—impacts the absorption properties of a molecule. Auxochromes, including hydroxyl (-OH) and amino ($-NH_2$) groups, also alter absorption by shifting wavelengths or enhancing intensity.

One of the most useful features of UV-Vis spectroscopy is its capacity to translate molecular structures from the wavelength of maximum absorption (λmax). A λmax shift may reflect structural alteration, solvent effects, or electronic interactions within the molecule. A bathochromic shift (red shift) is observed when λmax shifts to a longer wavelength as a result of extended conjugation or solvent polarity, whereas a hypsochromic shift (blue shift) yields a shift toward shorter wavelengths by steric effects or solvent interaction. Hyperchromic and hypochromic effects refer to changes in intensity of absorption owing to structural alteration.

A UV-Vis spectroscopy device contains a light source (typically a deuterium or tungsten lamp) which emits ultraviolet (UV) light, a monochromator to pick out individual wavelengths, a sample holder (most commonly a quartz cuvette), and a detector (e.g., photodiode or photomultiplier tube) to quantify the light absorbed. The device measures how much UV light is absorbed at various wavelengths by a sample and produces an absorption spectrum.

In general, UV-Vis spectroscopy is applied extensively in chemistry, biochemistry, and pharmaceuticals for the identification of organic

compounds, reaction mechanism studies, and molecular interaction monitoring. Its capacity to offer quick, non-destructive analysis makes it a fundamental tool for molecular interpretation and structural elucidation.

The adsorption and photo degradation studies of prepared electrospun membrane are examined using PerkinElmer UV/Vis Lambda 365. The analysis is taken within the wavelength 400-800.

Fig. 3.9. UV-Visible spectrometer (PerkinElmer Lambda 365, US).

3.8 PHOTOCATALYTIC STUDIES

To evaluate the adsorption capacity and photocatalytic performance of the electrospun membranes, 25 mg of the membrane sample was immersed in 50 mL of a 5-ppm methylene blue (MB) solution. The solution was stirred for 30 minutes in the dark to reach adsorption-desorption equilibrium. Thereafter exposed to visible light illumination using a Newport Corporation light source (USA) to examine the photocatalytic degradation

behavior. Aliquots were withdrawn at 30-minute intervals, and their absorbance was measured using a Lambda 365 UV-Vis spectrophotometer. The photocatalytic degradation efficiency (%) of methylene blue was determined using the equation: Degradation (%) = $(C_0 - C_t)/C_0\}*100$, where C_0 is the initial concentration of MB solution, and C_t is the concentration at time t. Similarly, adsorption studies are done by stirring the membranes in MB solution under dark for 3 h, with similar aliquot withdrawal and absorbance study.

Fig 3.10. Photo degradation studies done using solar stimulator (SAN-EI Electric, Japan)

Chapter 4

Results and discussion

4.1 CHARACTERIZATION OF ZnO, MXene, ZnO/MXene PHOTOCATALYST

4..1.1 XRD

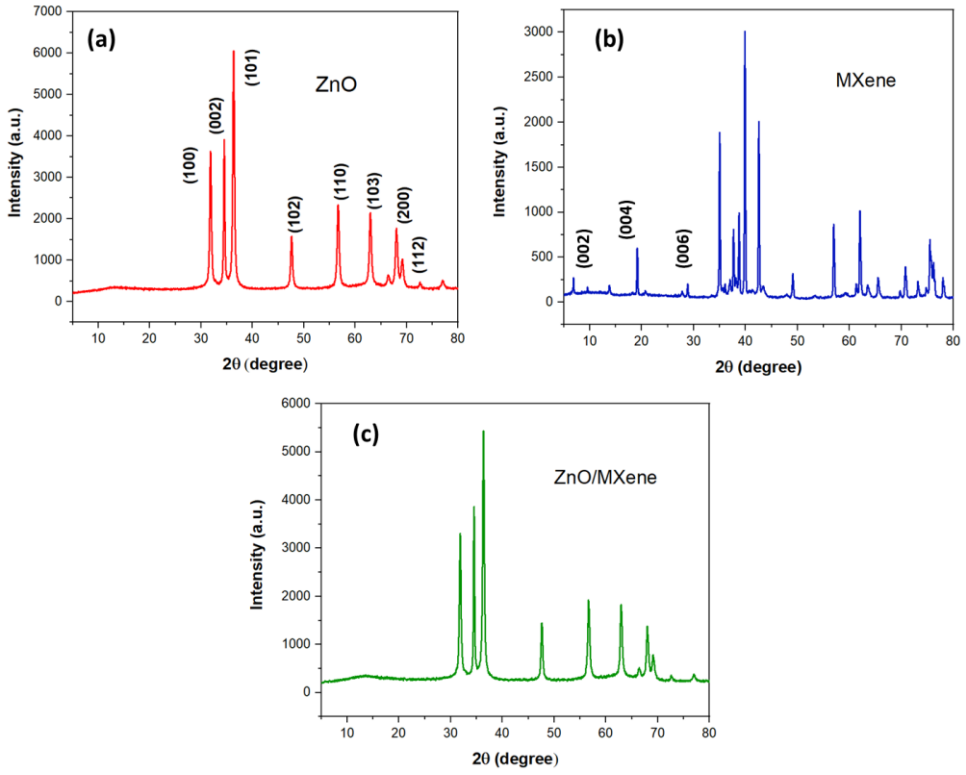

Fig 4.1 X-ray diffractograms of as-synthesized (a) ZnO, (b) MXene, and (c) ZnO/MXene.

Figure (a) shows the X-ray diffraction (XRD) pattern of the synthesized ZnO sample. The diffraction peaks are observed at characteristic 2θ positions, which correspond to the (100), (002), (101), (102), (110), (103), (200), and (112) planes of ZnO. These peak positions are in good agreement with the standard diffraction data for hexagonal wurtzite ZnO (JCPDS Card No. 36-1451). The presence of these peaks and the absence of any additional peaks indicate the phase purity of ZnO, confirming that no secondary phases such as $Zn(OH)_2$ are present in the sample. The peak corresponding to the (101) plane at approximately 36.2° exhibits the highest intensity, indicating that the ZnO crystallites have a preferential orientation along this plane. The peaks at 31.8° and 34.4°, corresponding to the (100) and (002) planes, respectively, also show significant intensity. The presence of these peaks suggests a polycrystalline nature with a well-formed wurtzite structure. The sharp and well-defined peaks observed in the XRD pattern indicate that the ZnO sample possesses a high degree of crystallinity. The broadening of the diffraction peaks is typically associated with small crystallite sizes or microstrain effects within the material. The presence of sharp peaks and the absence of amorphous humps suggest that the ZnO sample has well-developed grains with minimal structural defects. The wurtzite structure of ZnO is well-known for its wide direct band gap (~3.37 eV) and high exciton binding energy (~60 meV). The XRD analysis confirms the successful synthesis of phase-pure ZnO with a hexagonal wurtzite structure. The diffraction peaks match well with standard ZnO data, indicating high crystallinity and a preferred orientation along the (101) plane.

Figure (b) presents the X-ray diffraction (XRD) pattern of the synthesized MXene sample. The diffraction peaks observed at low angles, particularly

at 2θ ≈ 6.8°, 13°, and 19.1°, correspond to the (002), (004), and (006) planes, respectively. These peaks indicate the successful synthesis of a layered MXene structure. The presence of sharp and well-defined peaks suggests a crystalline nature of the material. The low-angle (002) reflection is a characteristic feature of MXene, signifying an interlayer spacing that depends on surface terminations (e.g., –OH, –F, –O groups) and hydration effects. The shift in the (002) peak position compared to pristine MAX phase $Ti_3 AlC_2$ suggests the selective removal of aluminum (Al) and the formation of a two-dimensional (2D) MXene structure. The multiple peaks in the high-angle region (above 30°) correspond to the basal planes of MXene, confirming the ordered stacking of 2D layers. However, if these peaks exhibit broadening, it indicates reduced layer stacking and increased exfoliation, leading to few-layer or single-layer MXene sheets. The intensity and sharpness of the (002) peak are directly correlated with the degree of oxidation and layer stacking order. A lower intensity or peak broadening suggests partial oxidation, which is a critical factor in MXene stability. If the (002) peak shifts towards a higher 2θ value, it indicates a decrease in interlayer spacing due to restacking or removal of intercalated species. A shift to a lower 2θ value suggests hydration or intercalation of larger molecules (e.g., polymers, ions). The presence of additional impurity peaks could indicate incomplete etching of the MAX phase or formation of secondary phases like TiO_2 , but no such impurities are evident in this spectrum, confirming the high purity of the synthesized MXene. The XRD analysis confirms the successful synthesis of MXene with well-defined (002), (004), and (006) peaks, characteristic of a layered structure.

Figure (c) shows the X-ray diffraction (XRD) pattern of the ZnO/MXene nanocomposite. The diffraction peaks observed correspond to the characteristic reflections of both ZnO and MXene, confirming the successful formation of the composite. The major peaks at $2\theta \approx 31.7°$, 34.4°, 36.2°, 47.5°, 56.6°, 62.8°, 67.9°, and 69.1° correspond to the (100), (002), (101), (102), (110), (103), (200), and (112) planes of hexagonal wurtzite ZnO (JCPDS No. 36-1451).The presence of the low-angle (002) peak from MXene around 6.5°, though weak, confirms the retention of the layered MXene structure. The intensity of this peak might have decreased due to the interaction of ZnO nanoparticles with MXene layers.The diffraction pattern confirms that ZnO nanoparticles are successfully incorporated into the MXene matrix without significantly altering their crystal structure. The incorporation of MXene into ZnO can influence the crystallite size, strain, and defect concentration of ZnO. The broadening of ZnO peaks in the composite compared to pure ZnO (Figure a) suggests: A possible reduction in crystallite size due to the restriction of ZnO grain growth by MXene layers. Increased structural disorder and strain, which could affect the electronic and optical properties of the composite.The presence of both ZnO and MXene peaks in the composite suggests a strong interfacial interaction. Possible interactions include:Charge transfer between ZnO and MXene: MXene's metallic conductivity can facilitate electron transport from ZnO, reducing recombination in photocatalytic or sensing applications.Possible MXene oxidation: The absence of new impurity peaks (e.g., TiO_2) suggests that MXene remained stable during the composite formation. However, a small shift in the (002) peak position could indicate partial oxidation or intercalation of ZnO nanoparticles within MXene layers.Compared to pure ZnO (Figure a), the composite shows slight peak broadening, suggesting smaller crystallite

sizes.Compared to pure MXene (Figure b), the characteristic low-angle (002) peak is weakened, indicating partial intercalation of ZnO.These structural changes indicate a synergistic effect, where MXene stabilizes ZnO nanoparticles while ZnO modifies the layered MXene structure.The XRD pattern confirms the successful formation of a ZnO/MXene composite with well-preserved crystallinity of both components.The reduction in ZnO crystallite size and possible strain effects may enhance its photocatalytic, gas sensing, and energy storage properties.

Sample	**Major peaks**	**Crystal structure**	**Key observations**
ZnO	31.7°, 34.4°, 36.2°, 47.5°, 56.6°, 62.8°, 67.9°, and 69.1°	Hexagonal Wurtzite	Sharp peaks indicate high crystallinity.
MXene	6.8°, 13°, and 19.1°	Layered structure	Low angle peaks (002) confirms MXene interlayer spacing.
ZnO/MXene	ZnO+Reduced MXene peaks	Composite	Reduced ZnO peak intensity, MXene peak suppression

Table 1: Comparative XRD analysis of ZnO, MXene, ZMX.

4.1.2. RAMAN analysis

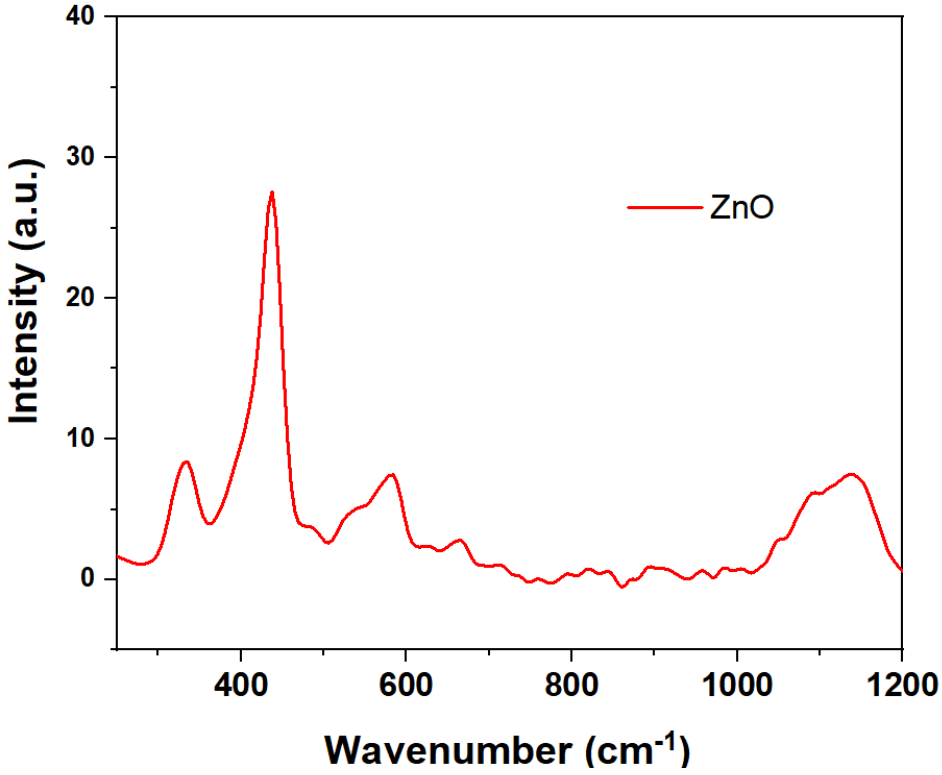

Figure 4.2. Raman spectra of as-synthesized ZnO nanoparticles.

The Raman spectrum of ZnO (Figure 4.2) exhibits characteristic vibrational modes, with a prominent peak around 437 cm^{-1} (E_2 (high)), confirming the wurtzite phase of ZnO. Additional peaks at ~99 cm^{-1} (E_2 (low)) and weaker multiphonon features near 330 cm^{-1} and 1150 cm^{-1} further validate its structural integrity. The strong intensity of the E_2 (high) mode indicates good crystallinity, while the presence of minor defect-related peaks suggests possible surface defects or strain effects.

Overall, the spectrum confirms the successful synthesis of ZnO with well-preserved vibrational characteristics.

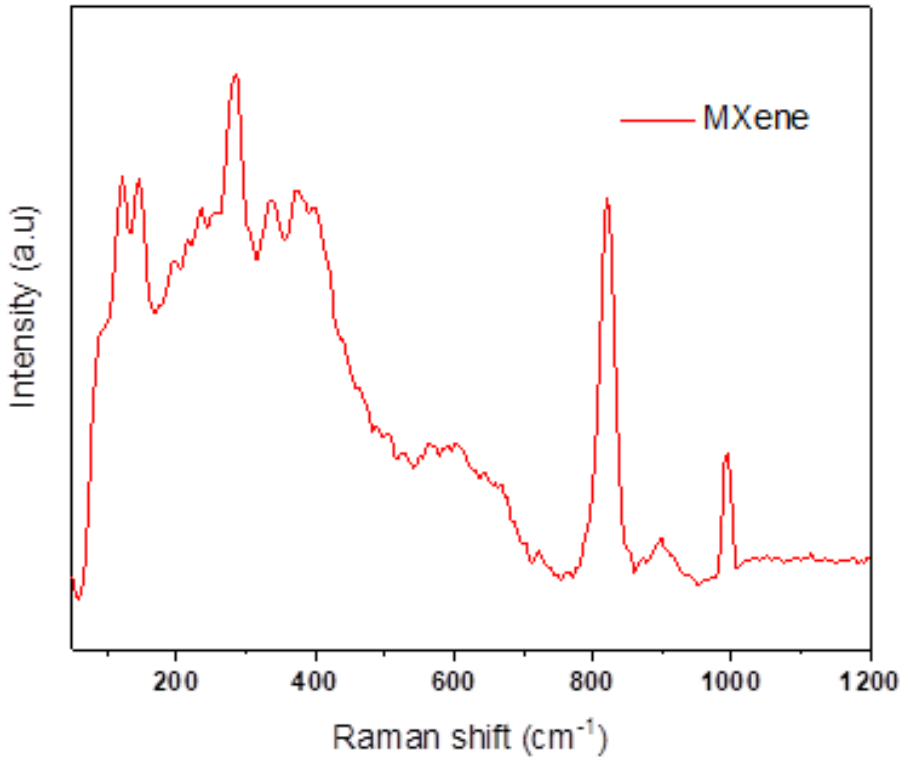

Fig 4.3 Raman spectra of MXene

The Raman spectrum of Mo_2TiC_2 MXene displays multiple characteristic peaks corresponding to its layered structure and surface terminations. In the low-wavenumber region (~150–300 cm^{-1}), prominent peaks are associated with M-A (Mo-Ti) vibrations and out-of-plane bending modes of the MXene layers, indicating the retention of its 2D layered morphology. The mid-wavenumber region (300–800 cm^{-1}) contains bands corresponding to in-plane vibrations of metal-carbon bonds (Mo-C and Ti-C stretching modes), confirming the preservation of the carbide

backbone. A strong peak near 800 cm^{-1} corresponds to the A_1 g vibration mode of Mo associated with surface functionalization (such as –OH, –F, and –O groups), which commonly occur due to the etching process used in MXene synthesis. Additional peaks in the higher wavenumber region (~1000 cm^{-1} and above) are indicative of oxygen-related vibrations and possible oxidation effects, a common phenomenon in air-exposed MXenes. These features suggest that some Mo and Ti atoms have partial oxidation, forming terminal bonds with oxygen-containing species, which can impact MXene's electrical and electrochemical properties. The broad nature of some peaks also indicates disorder and structural variations introduced during synthesis or due to interactions with functional groups.

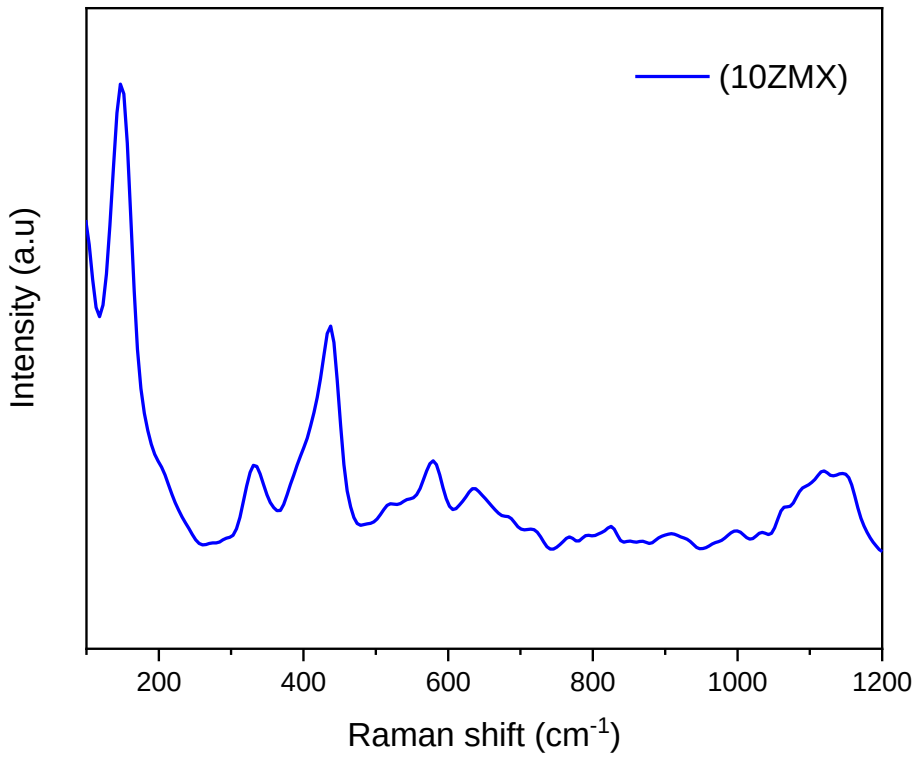

Fig 4.4. Raman spectra of 10%ZMX.

The Raman spectrum of the (10%ZMX) sample exhibits distinct peaks across the measured wavenumber range, indicating the presence of characteristic vibrational modes. A comparative analysis with typical MXene-based materials suggests possible structural modifications, phase compositions, and surface functionalities. Low-Wavenumber Region (100–400 cm^{-1}) The spectrum displays a strong peak around ~200 cm^{-1}, which is a characteristic feature of metal-carbon (M–C) vibrations. This peak suggests that the sample retains a structural framework similar to MXene, with transition metal-based vibrations dominating this region. Additional smaller peaks in this region indicate possible contributions from out-of-plane vibrations of the transition metal and interactions with terminating groups (such as -O, -OH, or -F). A set of moderate-intensity peaks is observed around ~500–700 cm^{-1}, which are commonly associated with metal-oxygen (M–O) vibrations. The broadness of peaks in this region suggests disorder or multiple functionalization states on the MXene surface. This could indicate partial oxidation or a mixture of M–O and M–C vibrations, depending on synthesis conditions.(53)

4.2 Characterisation of membranes based PCL, PCL/MXene,PCl/ZMX

4.2.1 SEM

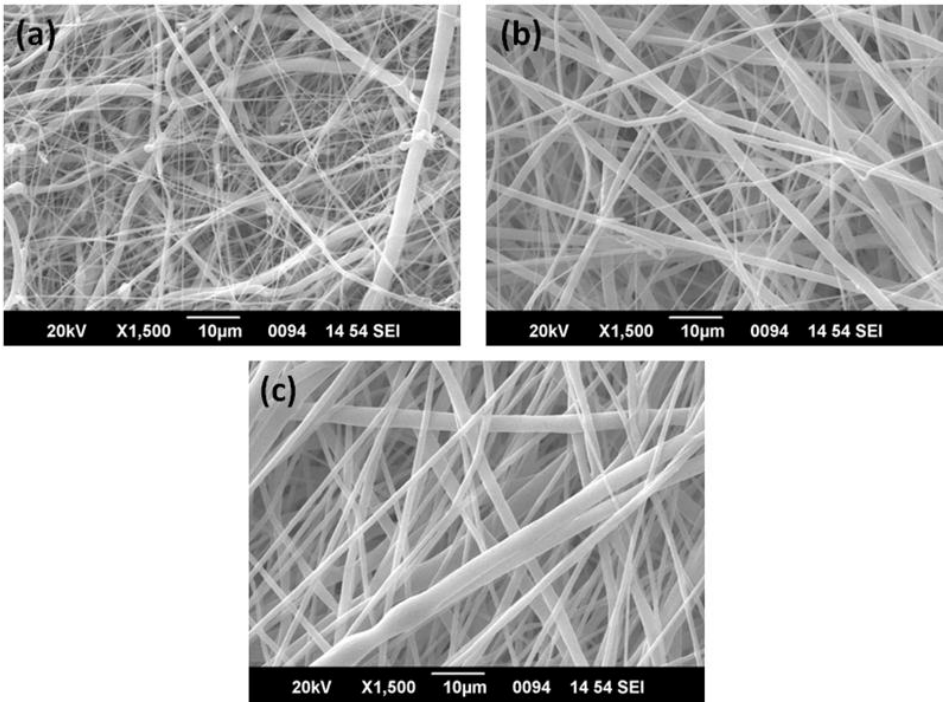

Fig 4.5. FESEM images of electrospun membranes: (a) PCL alone, (b) PCL/MXene, and (c) PCL/ZMX.

Field Emission Scanning Electron Microscopy (FESEM) was employed to investigate the morphological characteristics of the electrospun membranes. The obtained FESEM images (Figure 4.5) provide a detailed comparison of fiber morphology across different compositions: (a) PCL alone, (b) PCL/MXene, and (c) PCL/ZnO-MXene composite. The primary focus of the analysis is on fiber diameter distribution, alignment, bead

formation, and the influence of filler materials on the electrospinning process.

The pure PCL membrane (Figure 4.5a) exhibits a well-organized, interconnected fibrous network with relatively uniform fiber diameters and smooth surfaces. The fibers appear to be homogeneously distributed with minimal bead formation, suggesting that the electrospinning parameters (polymer concentration, applied voltage, and flow rate) were well optimized. The absence of significant beading implies a stable polymer jet during electrospinning, ensuring continuous fiber elongation and solidification before deposition. Additionally, the smooth surface morphology of the fibers suggests efficient polymer chain entanglement and stable jet stretching.

Upon the incorporation of MXene nanoparticles into the PCL matrix, a noticeable increase in fiber diameter is observed in Figure 4.5b. The fibers appear slightly thicker and more randomly oriented, with a wider diameter distribution compared to pure PCL. The mean fiber diameter has increased compared to neat PCL, and some degree of bead formation can be observed. The presence of small, spherical bead-like structures along the fibers suggests a partial disruption of the electrospinning process due to the introduction of MXene. The Increase in fiber diameter is likely attributed to the enhanced electrical conductivity of the electrospinning solution due to the presence of MXene nanosheets. Conductive fillers such as MXene can influence the charge distribution along the polymer jet, affecting its elongation and subsequent solidification. The moderate bead formation may be due to variations in solution viscosity, electrical conductivity, and charge repulsion during fiber formation. While the fibers in PCL/MXene exhibit greater structural variability, the improved

electrical conductivity of the composite could be advantageous for applications requiring enhanced electrochemical performance.

The most pronounced morphological changes are observed in Figure 4.5c. where ZnO/MXene fillers are incorporated into the polymer solution. The fibers exhibit a significant increase in diameter, with an exceptionally broad diameter distribution. Additionally, the presence of large bead structures is evident, suggesting a less stable electrospinning process. The significant fiber diameter variation in the PCL/ZnO-MXene composite is likely due to ZnO nanoparticle aggregation, which alters the viscosity and electrical conductivity of the polymer solution. ZnO/MXene composites tend to form strong hydrogen bonding interactions with the PCL matrix, potentially leading to polymer chain entanglement that disrupts smooth fiber formation.Despite the increased bead formation, the rougher surface texture and broader fiber diameter distribution in PCL/ZnO-MXene membranes may be beneficial for applications where increased surface area and porosity are desired, such as filtration, antibacterial coatings, and photocatalytic application. Bead formation is a critical parameter in electrospinning, as it affects the mechanical integrity, porosity, and overall performance of the electrospun membranes. The presence of beads is generally considered a defect, as it indicates an unstable electrospinning process.

From the comparative analysis, it is evident that the incorporation of MXene and ZnO/MXene into the PCL matrix alters fiber morphology by increasing fiber diameter and inducing bead formation. These modifications suggest that filler materials affect the rheological properties of the polymer solution, which in turn influence fiber formation during electrospinning. While the neat PCL membrane exhibits smooth and uniform fibers, the inclusion of MXene and ZnO/MXene results in

increased heterogeneity, which could be beneficial in applications requiring tunable surface properties.

Parameter	**PCL alone**	**PCL/MXene**	**PCL/ZMX**
Fiber Alignment	Well organized, interconnected network	Slightly disordered, less alignment	Highly disordered, randomly oriented
Fiber Diameter	Small and uniform	Increased, moderate variability	Widest diameter, highly variable
Fiber Surface	Smooth and continuous	Slightly rough due to MXene interaction	Rougher surface due to ZnO/MXene presence
Bead Formation	Minimal	Some bead formation	Pronounced bead formation

Table 2: FESEM comparative studies of PCL, PCL/MXene, PCL/ZMX membrane.

4.3 DEGRADATION STUDIES

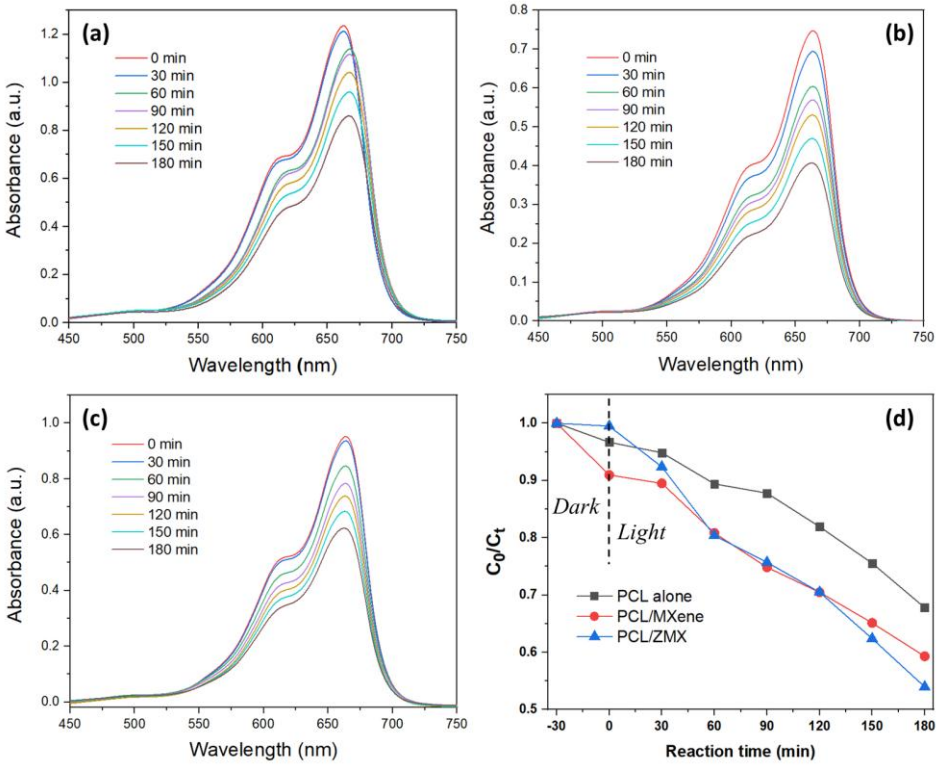

Figure 4.6. UV-Vis absorbance spectra of MB in presence of (a) PCL Membrane, (b) PCL/MXene Membrane, and (c) PCL/ZMX Membrane at different intervals of time. (d) Photodegradation plot of MB in presence of membranes with respect to time.

Photocatalytic and Adsorption Performance of PCL-Based Hybrid Membranes Incorporating ZnO/MXene for Methylene Blue Removal is studied by UV-Vis spectroscopy.The presence of organic pollutants, such as methylene blue (MB), in wastewater necessitates the development of efficient removal strategies. Hybrid membranes combining polymeric

materials with nanostructured photocatalysts offer a promising approach to improve pollutant degradation. In this study, polycaprolactone (PCL) membranes were modified with MXene nanosheets and ZnO/MXene (ZMX) composites to enhance both adsorption and photocatalytic degradation. The UV-Vis spectral analysis over a reaction period of 180 minutes provides insights into the MB removal efficiency of these membranes. The UV-Vis absorption spectra (Figure 4.6a–c) reveal the degradation kinetics of MB in the presence of different membranes.

Figure 4.6(a) – PCL Membrane:The characteristic MB absorption peak at ~665 nm declines slowly over time. The PCL membrane alone lacks photocatalytic activity, leading to limited degradation efficiency of 32% after 180 minutes.This suggests that MB removal occurs primarily through weak adsorption rather than photocatalysis .Figure 4.6(b) – PCL/MXene Membrane:A moderate reduction in MB absorbance is observed, indicating enhanced degradation compared to PCL alone.MXene nanosheets introduce additional active sites, facilitating charge separation and improving photocatalytic performance.The degradation efficiency reaches 41%, confirming MXene's role in accelerating MB degradation. Figure 4.6(c) – PCL/ZnO/MXene (ZMX) Membrane: The sharpest decline in absorbance is observed, indicating rapid and efficient MB degradation. The ZnO nanoparticles on MXene provide additional active sites and enhance light absorption through synergistic ZnO-MXene interactions. The PCL/ZMX membrane achieves the highest degradation efficiency of 46%, outperforming both PCL and PCL/MXene membranes. Before light irradiation, adsorption experiments were conducted to evaluate MB removal in the dark phase:PCL membrane alone showed negligible adsorption (3%), highlighting its poor dye affinity.PCL/MXene exhibited

the highest adsorption efficiency (47.5%), attributed to the high surface area and hydrophilic functional groups of MXene. PCL/ZMX demonstrated an adsorption efficiency of 30.8%, lower than PCL/MXene but still significantly higher than PCL alone.These findings indicate that MXene-dominated membranes favor adsorption, whereas ZnO/MXene membranes prioritize photocatalytic degradation.Figure 4.6(d) presents the C_0 /Ct vs. reaction time data:Dark phase:PCL/MXene shows the highest initial MB adsorption. PCL/ZMX exhibits moderate adsorption but rapid MB removal upon light exposure.Light phase:PCL/ZMX shows the fastest degradation rate, demonstrating superior photocatalytic performance due to ZnO's high electron mobility and MXene's charge transfer properties. PCL/MXene balances adsorption and photocatalysis, making it effective for sustained MB removal. PCL alone remains the least effective, reaffirming its limited photocatalytic activity.

The enhanced photocatalytic and adsorption properties of PCL-based hybrid membranes arise from:-MXene's high surface area and functionalized sites, which promote strong MB adsorption . ZnO's role in PCL/ZMX, introducing additional active sites for charge separation and enhanced light absorption. The synergistic ZnO-MXene interaction, leading to enhanced electron mobility, reduced recombination, and superior photocatalysis. PCL/ZnO/MXene (PCL/ZMX) demonstrated the highest photocatalytic degradation efficiency (46%), making it ideal for light-driven MB removal.PCL/MXene exhibited superior adsorption efficiency (47.5%), highlighting its potential for dye adsorption applications. PCL alone showed minimal MB removal efficiency, reinforcing the need for nanostructured additives. ZnO incorporation enhances charge transfer and light absorption, improving photocatalytic

efficiency. These results suggest that PCL/ZMX is optimal for photocatalytic degradation, while PCL/MXene is better suited for adsorption-based applications.

Property	PCL alone	PCL/MXene	PCL/ZMX
Photocatalytic Degradation	32%	41%	46%
Primary Mechanism	Minimal photodegradation due to the lack of actve sites	Enhace charge separation on via MXene conductive pathways	Synergistic effect of ZnO and MXene
Adsorption Efficiency	3%	47.5%	30.8%
Adsorption Mechanism	Weak phyiscal adsorption	MXene driven adsorption on via electrostatic interaction	Moderate adsorption + photocatalysis

Table 3: Photocatalytic degradation and adsorption efficiency of PCL alone, PCL/MXene, PCL/ZMX Membrane.

Chapter 5

Conclusions

The results obtained from the XRD studies confirms the successful synthesis of ZnO/MXene hybrids from the data obtained from the 2θ values corresponding to the different peaks in the data, this data was analyzed from the experimental data done before. There was absence of unwanted peaks which actually reveals the purity of the compound and integrating them into PCL membranes via electrospinning for water treatment applications. XRD analysis confirmed the crystalline integrity of ZnO in the hybrids and the successful exfoliation of MXene. Morphological studies were conducted which showed the presence of fibrous alignment in all the three memebrane synthesized, there was substantial changes in the membrane with the incorporation of the hybrids. There was an increase in the number of beads formed so as an increase the diameter of the fiber. The texture of the membrane also changed with the addition of hybrids, the surface of the hybrids was rougher due to the interation of MXene and MXene/ZNO. Photocatalytic tests demonstrated superior degradation efficiency for the PCL/ZMX membrane (46%), this was due the moderate adsorption and photocatalysis, highlighting its potential in pollutant degradation. Meanwhile, the PCL/MXene membrane exhibited excellent adsorption efficiency (47.5%), this was due to its adsorption alone because it has more surface area, making it ideal for dye adsorption. These findings underscore the dual functionality of MXene-based membranes for advanced water purification strategies.

References

1. Gogotsi Y, Anasori B. The Rise of MXenes. ACS Nano [Internet]. 2019 Aug 27 [cited 2025 Feb 21];13(8):8491–4. Available from: https://pubs.acs.org/doi/full/10.1021/acsnano.9b06394

2. Dwivedi S, Shikha D. Water pollution: Causes, effects and control. Biochem Cell Arch. 2016;16.

3. Cost of Color: Textile Dyeing Industry Polluting Asian Rivers [Internet]. [cited 2025 Feb 20]. Available from: https://www.planetcustodian.com/dyeing-industry-polluting-asian-rivers/15641/

4. Goel PK. Water pollution: causes, effects and control. New age international; 2006.

5. Rad SM, Ray AK, Barghi S. Water Pollution and Agriculture Pesticide. Vol. 4, Clean Technologies. 2022.

6. Rajasulochana P, Preethy V. Comparison on efficiency of various techniques in treatment of waste and sewage water–A comprehensive review. Resource-Efficient Technologies. 2016;2(4):175–84.

7. Lusweti E, Kanda EK, Obando J, Makokha M. Effects of oil exploration on surface water quality – a review. Vol. 17, Water Practice and Technology. 2022.

8. Risks to health from water pollution | Download Scientific Diagram [Internet]. [cited 2025 Feb 20]. Available from: https://www.researchgate.net/figure/Risks-to-health-from-water-pollution_fig23_269400117

9. Lin L, Yang H, Xu X. Effects of Water Pollution on Human Health and Disease Heterogeneity: A Review. Vol. 10, Frontiers in Environmental Science. 2022.

10. Schwarzenbach RP, Egli T, Hofstetter TB, Von Gunten U, Wehrli B. Global water pollution and human health. Annu Rev Environ Resour. 2010;35(1):109–36.

11. Warsi AZ, Aziz F, Zulfiqar S, Haider S, Shakir I, Agboola PO. Synthesis, Characterization, Photocatalysis, and Antibacterial Study of WO3, MXene and WO3/MXene Nanocomposite. Nanomaterials. 2022;12(4).

12. Ângelo J, Andrade L, Madeira LM, Mendes A. An overview of photocatalysis phenomena applied to NOx abatement. J Environ Manage. 2013 Nov 15;129:522–39.

13. Lim H, Yusuf M, Song S, Park S, Park KH. Efficient photocatalytic degradation of dyes using photo-deposited Ag nanoparticles on ZnO structures: simple morphological control of ZnO. RSC Adv. 2021;11(15).

14. Louis J, Padmanabhan NT, Jayaraj MK, John H. Crystal lattice engineering in a screw-dislocated ZnO nanocone photocatalyst by carbon doping. Mater Adv [Internet]. 2022;3(10):4322–33. Available from: http://dx.doi.org/10.1039/D2MA00098A

15. Klingshirn C. ZnO: material, physics and applications. ChemPhysChem. 2007;8(6):782–803.

16. Lee JH, Ko KH, Park BO. Electrical and optical properties of ZnO transparent conducting films by the sol-gel method. J Cryst Growth. 2003;247(1–2).

17. Ravichandran K, Sindhuja E. Fabrication of cost effective g-C3N4+Ag activated ZnO photocatalyst in thin film form for enhanced visible light responsive dye degradation. Mater Chem Phys. 2019;221.

18. Lei JC, Zhang X, Zhou Z. Recent advances in MXene: Preparation, properties, and applications. Vol. 10, Frontiers of Physics. 2015.

19. Deshmukh K, Muzaffar A, Kovárík T, Ahamed MB, Pasha SKK. Introduction to 2D MXenes: fundamental aspects, MAX phases and MXene derivatives, current challenges, and future prospects. MXenes and their Composites: Synthesis, Properties and Potential Applications. 2022 Jan 1;1–47.

20. Lim KRG, Shekhirev M, Wyatt BC, Anasori B, Gogotsi Y, Seh ZW. Fundamentals of MXene synthesis. Nature Synthesis. 2022;1(8):601–14.

21. Persson POÅ, Rosen J. Current state of the art on tailoring the MXene composition, structure, and surface chemistry. Curr Opin Solid State Mater Sci. 2019;23(6):100774.

22. Alam MS, Chowdhury MA, Khandaker T, Hossain MS, Islam MS, Islam MM, et al. Advancements in MAX phase materials: structure, properties, and novel applications. RSC Adv. 2024 Aug 27;14(37):26995–7041.

23. Khazaei M, Ranjbar A, Arai M, Sasaki T, Yunoki S. Electronic properties and applications of MXenes: a theoretical review. J Mater Chem C Mater. 2017;5(10):2488–503.

24. Hantanasirisakul K, Gogotsi Y. Electronic and optical properties of 2D transition metal carbides and nitrides (MXenes). Advanced materials. 2018;30(52):1804779.

25. Yu L, Xu L, Lu L, Alhalili Z, Zhou X. Thermal properties of MXenes and relevant applications. ChemPhysChem. 2022;23(17):e202200203.

26. Guan Y, Zhang M, Qin J, Ma X, Li C, Tang J. Hydrophilicity-dependent distinct frictional behaviors of different modified MXene nanosheets. The Journal of Physical Chemistry C. 2020;124(25):13664–71.

27. Han M, Maleski K, Shuck CE, Yang Y, Glazar JT, Foucher AC, et al. Tailoring electronic and optical properties of MXenes through forming solid solutions. J Am Chem Soc. 2020;142(45):19110–8.

28. Fu B, Sun J, Wang C, Shang C, Xu L, Li J, et al. MXenes: Synthesis, optical properties, and applications in ultrafast photonics. Small. 2021;17(11):2006054.

29. Zeng W, Ye X, Dong Y, Zhang Y, Sun C, Zhang T, et al. MXene for photocatalysis and photothermal conversion: Synthesis, physicochemical properties, and applications. Coord Chem Rev. 2024;508:215753.

30. Xu D, Li Z, Li L, Wang J. Insights into the photothermal conversion of 2D MXene nanomaterials: synthesis, mechanism, and applications. Adv Funct Mater. 2020;30(47):2000712.

31. Mostafavi E, Iravani S. MXene-graphene composites: a perspective on biomedical potentials. Nanomicro Lett. 2022;14(1):130.

32. Awasthi GP, Maharjan B, Shrestha S, Bhattarai DP, Yoon D, Park CH, et al. Synthesis, characterizations, and biocompatibility evaluation of polycaprolactone–MXene electrospun fibers. Colloids Surf A Physicochem Eng Asp. 2020;586:124282.

33. Zhang L, Song W, Liu H, Ding H, Yan Y, Chen R. Influencing Factors on Synthesis and Properties of MXene: A Review. Vol. 10, Processes. 2022.

34. Kumar JA, Prakash P, Krithiga T, Amarnath DJ, Premkumar J, Rajamohan N, et al. Methods of synthesis, characteristics, and environmental applications of MXene: A comprehensive review. Chemosphere. 2022;286.

35. Lim KRG, Shekhirev M, Wyatt BC, Anasori B, Gogotsi Y, Seh ZW. Fundamentals of MXene synthesis. Nature Synthesis 2022 1:8 [Internet]. 2022 Aug 1 [cited 2025 Feb 21];1(8):601–14. Available from: https://www.nature.com/articles/s44160-022-00104-6

36. Thakur A, Chandran B.S. N, Davidson K, Bedford A, Fang H, Im Y, et al. Step-by-Step Guide for Synthesis and Delamination of Ti3C2Tx MXene. Small Methods. 2023;7(8).

37. Wang R, Li M, Sun K, Zhang Y, Li J, Bao W. Element- doped Mxenes: mechanism, synthesis, and applications. Small. 2022;18(25):2201740.

38. Lu C, Yang L, Yan B, Sun L, Zhang P, Zhang W, et al. Nitrogen- doped Ti3C2 MXene: mechanism investigation and electrochemical analysis. Adv Funct Mater. 2020;30(47):2000852.

39. Yoon J, Shin M, Lim J, Lee JY, Choi JW. Recent Advances in MXene Nanocomposite-Based Biosensors. Vol. 10, Biosensors. 2020.

40. Riazi H, Taghizadeh G, Soroush M. MXene-Based Nanocomposite Sensors. ACS Omega. 2021;6(17).

41. Rakhi RB, Nayuk P, Xia C, Alshareef HN. Novel amperometric glucose biosensor based on MXene nanocomposite. Sci Rep. 2016;6.

42. Im JK, Sohn EJ, Kim S, Jang M, Son A, Zoh KD, et al. Review of MXene-based nanocomposites for photocatalysis. Chemosphere. 2021;270:129478.

43. Riazi H, Taghizadeh G, Soroush M. MXene-based nanocomposite sensors. ACS Omega. 2021;6(17):11103–12.

44. Riazi H, Taghizadeh G, Soroush M. MXene-based nanocomposite sensors. ACS Omega. 2021;6(17):11103–12.

45. Bhardwaj R, Hazra A. MXene-based gas sensors. J Mater Chem C Mater. 2021;9(44):15735–54.

46. Ronchi RM, Arantes JT, Santos SF. Synthesis, structure, properties and applications of MXenes: Current status and perspectives. Ceram Int. 2019 Oct 15;45(15):18167–88.

47. Polycaprolactone (PCL) biodegradable polyester, chemical structure. Frequently used for biomedical applications and for rapid prototyping. Skeletal fo Stock Vector Image & Art - Alamy [Internet]. [cited 2025 Feb 21]. Available from: https://www.alamy.com/polycaprolactone-pcl-biodegradable-polyester-chemical-structure-frequently-used-for-biomedical-applications-and-for-rapid-prototyping-skeletal-fo-image216973677.html

48. Bezerra EB, França DC, De Souza Morais DD, De Freitas Rosa M, Morais JPS, Araújo EM, et al. Processing and properties of PCL/Cotton linter compounds. Materials Research. 2017;20(2).

49. 5 Properties of polycaprolactone. | Download Scientific Diagram [Internet]. [cited 2025 Feb 21]. Available from: https://www.researchgate.net/figure/Properties-of-polycaprolactone_fig2_348902304

50. Labet M, Thielemans W. Synthesis of polycaprolactone: a review. Chem Soc Rev. 2009 Nov 17;38(12):3484-504.

51. Mochane MJ, Motsoeneng TS, Sadiku ER, Mokhena TC, Sefadi JS. Morphology and properties of electrospun PCL and its composites for medical applications: A mini review. Vol. 9, Applied Sciences (Switzerland). 2019.

52. Louis J, Padmanabhan NT, Jayaraj MK, John H. Crystal lattice engineering in a screw-dislocated ZnO nanocone photocatalyst by carbon doping. Mater Adv [Internet]. 2022 May 23 [cited 2025 Feb

21];3(10):4322–33. Available from: https://pubs.rsc.org/en/content/articlehtml/2022/ma/d2ma00098a

53. Padmanabhan NT, Sabin C, Unni Krishnan H, Hrithik M, Mythili U, Jayaraj MK, et al. Analysing the efficacy of TiO2/g-C3N4 nanohybrid electrospun membranes for visible-light photocatalytic water purification. Chem Phys Lett. 2024 Nov 1;854.